TOPICAL REVIEW

Magnetic particle hyperthermia—a promising tumour therapy?

To cite this article: Silvio Dutz and Rudolf Hergt 2014 *Nanotechnology* **25** 452001

IOP Publishing Nanotechnology
Nanotechnology **25** (2014) 452001 (28pp) doi:10.1088/0957-4484/25/45/452001

Topical Review

Magnetic particle hyperthermia —a promising tumour therapy?

Silvio Dutz[1,2] **and Rudolf Hergt**[2]

[1] Institute of Biomedical Engineering and Informatics (BMTI), Technische Universität Ilmenau, G-Kirchhoff-Str. 2, D-98693 Ilmenau, Germany
[2] Department of Nano Biophotonics, Institute of Photonic Technology (IPHT), A.-Einstein-Str. 9, D-07745 Jena, Germany

E-mail: silvio.dutz@tu-ilmenau.de

Received 30 May 2014
Accepted for publication 29 July 2014
Published 22 October 2014

Abstract

We present a critical review of the state of the art of magnetic particle hyperthermia (MPH) as a minimal invasive tumour therapy. Magnetic principles of heating mechanisms are discussed with respect to the optimum choice of nanoparticle properties. In particular, the relation between superparamagnetic and ferrimagnetic single domain nanoparticles is clarified in order to choose the appropriate particle size distribution and the role of particle mobility for the relaxation path is discussed. Knowledge of the effect of particle properties for achieving high specific heating power provides necessary guidelines for development of nanoparticles tailored for tumour therapy. Nanoscale heat transfer processes are discussed with respect to the achievable temperature increase in cancer cells. The need to realize a well-controlled temperature distribution in tumour tissue represents the most serious problem of MPH, at present. Visionary concepts of particle administration, in particular by means of antibody targeting, are far from clinical practice, yet. On the basis of current knowledge of treating cancer by thermal damaging, this article elucidates possibilities, prospects, and challenges for establishment of MPH as a standard medical procedure.

Keywords: hyperthermia, magnetite, magnetic nanoparticles, tumour therapy, hysteresis

(Some figures may appear in colour only in the online journal)

1. Introduction

Medics have known of the healing effect of heat for different diseases for a long time. About 150 years ago, Busch found that tumours cease to grow for temperature above 42 °C whilst healthy tissue is not affected by such temperatures [33]. In more modern times the selective damage of tumour tissue by means of a local temperature increase is an approved and established cancer therapy [68, 221]. For this so-called hyperthermia there are several ways basing on different physical mechanisms to obtain temperatures suitable for cancer treatment within biological tissue. Prominent examples are microwave irradiation applied via radiofrequency antennas (dielectric heating) [53, 203, 206], Ohmic heating via electrode-applied high frequency currents [30, 36, 52, 141], optical laser irradiation via fibres [185] or water bath heating such as whole body hyperthermia [11, 182]. All of these techniques to realize therapeutically suitable temperatures suffer from one common basic disadvantage: the control of spatial extent of heating in tissue is still an unsolved challenging task.

Magnetic particle hyperthermia (MPH) enables real local heating by embedding the heating source (magnetic particles) into the tumour tissue and heating it by using an external alternating magnetic field. This means a clear improvement of therapy compared to other heating techniques. Almost 60 years ago Gilchrist *et al* [74] presented first experimental work on MPH. In this work resected lymph nodes of a dog

were heated up *ex vivo* by application of larger iron oxide particles into tumour and exposure of loaded tissue to alternating magnetic fields. Follow up these experiments, in the first years phantom studies and animal experiments were carried out to investigate performance of magnetic hyperthermia [29, 105, 120, 178]. In recent years, MPH has shown success in the first clinical trials [79, 117–119, 149] and advanced clinical trials are on the way. Outcome of these clinical trials demonstrated the efficacy of magnetic hyperthermia for prostate cancer and gliomas and showed that patients can tolerate this therapy without discomfort or serious side effects. An interesting work on different practical aspects for application of magnetic hyperthermia is presented by Ortega and Pankhurst [168].

Recent achievements of magnetic hyperthermia in cancer therapy are very promising but the method still needs further improvement before it can become a standard medical procedure [208]. In particular, two main tasks must be addressed: firstly, it is necessary to determine a safe, comfortable, and reproducible method of nanoparticle delivery to the tumour region. In addition to the realization of a reliable intratumoural injection, investigations into alternative methods include antibody targeting and resulting cellular uptake. Secondly, a further improvement of the specific heating power (SHP) of the magnetic nanoparticles (MNPs) is crucial to reach and maintain therapeutically suitable temperatures inside the tumour tissue with a minimum of magnetic material to be delivered to tumour.

The aim of the present article is to provide a comprehensive background on the physical and materials science aspects of MNP development for hyperthermia. The correlation between properties of used magnetic particles and resulting heating power shall be emphasized and expanded on. Additionally to particle properties measured on liquid ferrofluids we take into account boundary conditions for magnetic particle heating as they occur during real hyperthermia therapy experiments. As a consequence of these more realistic considerations, we shall discuss the future prospects and likely limitations of this promising cancer therapy.

2. Basics of magnetic particle heating

MPH is focused on the destruction of tumours by heat, which is generated by fine magnetic particles placed in the tumour tissue. In order to produce heat, the particles must be subjected to an alternating magnetic field that is generated by external coils situated outside of the patient's body. In principle, alternating magnetic fields induce eddy currents in any conducting medium. However, this mechanism of inductive heat production—though a widely used technique—is not suitable for nanoparticle heating in hyperthermia. There are two reasons: Firstly, induction heating relies on electrical conduction in the medium to be heated. However, electrical conductivity of magnetic iron oxides—which proved to be very useful for MPH—is rather low. Secondly, the induced electrical voltage is rather weak due to the extremely small dimensions of possible eddy current loops within a nanoparticle. So, a useful induction heating effect does not occur, not even in good electrically conducting metal particles—the suitability of which for MPH is rather questionable for other reasons. Thus, the terminus 'induction heating' found sometimes in literature with respect to application of MNPs in hyperthermia is misleading.

In contrast, the argument of too small current loops of course does not apply to the body of a human patient. There, the external alternating field may indeed induce considerable eddy currents in the body of a patient. This may have serious consequences, which will be considered below in discussing limitations of MPH. In comparison, tumour heating by means of MNPs relies mainly on a quite different, purely magnetic effect—on magnetic hysteresis losses in an external alternating magnetic field.

2.1. Magnetism of nanoparticles

The main source of heat generation in magnetic materials is by *hysteresis*. From an atomic point of view, magnetic hysteresis is caused by the coupling of the atomic spins to the crystal lattice. The resulting transfer of electromagnetic energy to the lattice in form of heat is quite undesirable in many technical applications of magnetic materials. Therefore, in these applications one often speaks of this energy transformation as *magnetic losses*. The amount of the energy loss per cycle is given by the area of the hysteresis loop which the particle magnetization undergoes if the external magnetic field is cycled over one period. The heating *power* is defined as energy per cycle times frequency f. Consequently, there is a general increase of power when the frequency of the alternating external field is raised. Besides this general linear frequency dependence, the shape of the hysteresis loop itself may depend essentially on field frequency, too. Accordingly, the effectiveness of a hyperthermia treatment apparatus depends crucially on the following technical parameters, namely the amplitude and frequency of the magnetic field. One should keep in mind that the generation of alternating magnetic fields of large amplitude and high frequency, e.g. by means of coils, offer a very real technical challenge. The necessary technical efforts increase seriously with increasing product of both magnitudes. Moreover, the required energy of a magnetic field increases remarkably with the spatial extension of the field. This, in itself, represents a considerable technical challenge when achieving large magnetic field strength in a large volume, e.g. the whole human body.

Apart from the magnetic hysteresis losses, a quite different loss type may occur in *fluid* magnetic suspensions: In this case, heat may be additionally generated by *viscous friction* which is caused by rotations or oscillations of particles induced by the external alternating field. We will discuss those so called Brownian losses in detail below, too. Since there are valuable reviews in literature referring to magnetic losses (e.g. [129]), we will restrict ourselves here on some topics of practical relevance for hyperthermia.

In this article, we use three terms to specify magnetic losses during the reversal of magnetization: The first of these is 'specific hysteresis loss' (SHL) which is measured under

quasistatic conditions in a magnetometer (hysteresis curve). There, the loop area will be normalized to sample mass. Multiplying the SHL with an applied frequency leads to the second term, 'specific loss power' (SLP). This gives an estimation of the third term, the 'SHP' which provides the real heating ability of the particles as determined by thermal measurement on the samples of the particles exposed to an alternating magnetic field.

2.1.1. Magnetic hysteresis. The hysteresis loop of magnetic materials is characterized mainly by three typical material dependent parameters: *Saturation magnetization* M_S is the maximum magnetization that may be achieved by increasing the external magnetic field—besides a very weak linear contribution called paramagnetism. The field value required to achieve this is termed saturation field. After removing the external field a *remanent magnetization* M_R is, in general, left over. In order to remove that remanence, a reversed external field must be applied, which is called *coercivity* H_C. All these parameters are important for the heat output of nanoparticles and may vary considerably for different particle types. Of particular interest is the coercivity since below that field strength no reversal of the magnetization and accordingly no hysteresis losses may occur.

In macroscopic samples of magnetic materials, *magnetic domains* typically exist and are separated by domain walls (see *textbooks of magnetism* e.g. [129]). However, this so-called multidomain state will become energetically unfavourable below a defined particle size. Then, each particle represents a single magnetic domain. Both domain states differ essentially with respect to the microscopic processes of magnetization reversal. In multidomain particles the reversal of the magnetization direction takes place via domain wall displacement. The energy barriers against that wall movement are relatively small in comparison to the reversal of the complete magnetic moment of a single domain particle. Accordingly, multidomain particles are magnetically much 'softer' than single domain particles and consequently exhibit comparatively low hysteresis loss. In single domain particles the magnetic moment has to be rotated against an energy barrier given mainly by *anisotropy K* due to the crystal lattice and the particle shape. For magnetite, which is presently considered as the most favourable material for MPH, the transition between multidomain and single domain state occurs at about 30 nm particle diameter [94].

Of course, the most important physical parameter of a MNP system for hyperthermia is its heating power which should be delivered by a minimal amount of material. As a rough measure for maximum hysteresis loss, the product $(M_R \cdot H_C)$ may be taken. A comprehensive survey on modern results may be found in '*Micromagnetism and the Microstructure of Ferromagnetic Solids' by Kronmüller and Fähnle* [129]. The special case of an ensemble of aligned, uniaxial, homogeneously magnetized ellipsoidal particles was theoretically treated in the famous classical paper of Stoner and Wohlfarth [202]. This represents an ideal system and as such a material consisting of so-called Stoner–Wohlfarth-particles

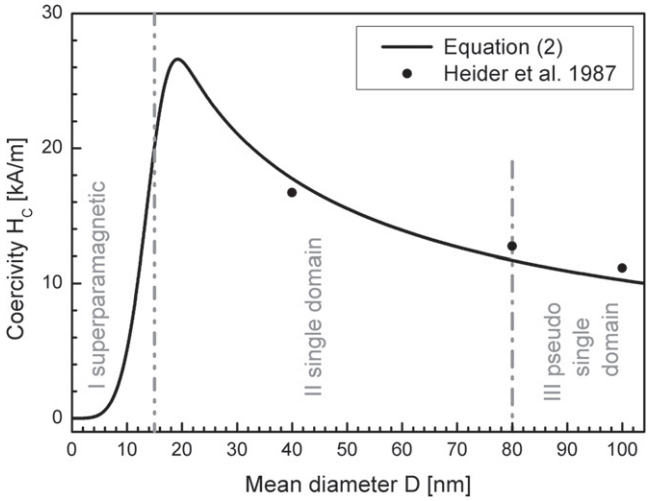

Figure 1. Dependence of the coercivity of maghemite nanoparticles on particle size, from [98] © IOP Publishing. Reproduced by permission of IOP Publishing. All rights reserved.

would deliver the highest amount of hysteresis energy possible. With all particle axes parallel to the field direction, a rectangular hysteresis loop is observed which gives a maximum hysteresis loss density according to:

$$Q = 4\mu_0 \cdot M_S \cdot H_C \left(\mathrm{Jm^{-3}}\right) \text{ with } \mu_O = 4\pi 10^{-7} \left(\mathrm{Vs\ Am^{-1}}\right). \quad (1)$$

The SLP is given by

$$\mathrm{SLP} = \frac{Q \cdot f}{\rho} = \mathrm{SHL} \cdot f \left(\mathrm{W\ kg^{-1}}\right), \quad (1a)$$

where ρ is the mass density. This loss occurs only if the external field exceeds the coercivity field. Otherwise nearly no reversal of the magnetic moments may occur and consequently loss is negligibly small. For example, in the case of magnetite (Fe_3O_4, $M_S = 480\ \mathrm{kA\ m^{-1}}$, $H_C = 30\ \mathrm{kA\ m^{-1}}$, $\rho = 5240\ \mathrm{kg\ m^{-3}}$) using a technically achievable frequency of $f = 500$ kHz one may estimate a rather large SLP of $7\ \mathrm{kW\ g^{-1}}$. However, in practice this large amount of heating power is rarely realized due to several limitations.

The most important, but somewhat intriguing material parameter of a magnetic particle ensemble is the coercivity. In general, coercivity H_C as well as remanence M_R *increases* with *decreasing* particle size. In the past, the dependence of coercivity on particle size was the subject of a lot of papers, in particular in relation to applications of magnetic particles for recording technologies (see [151]). Valuable experimental investigations on magnetite particles are due to Heider *et al* [94]. The latter results show that coercivity is a structure dependent parameter which, in particular, is different for well crystallized particles in contrast to particles produced by grinding. Maghemite particles for hyperthermia application are mainly produced by different forms of chemical precipitation and growth techniques to be described below. In general, those particles show a rather undisturbed crystal lattice as proved by various investigations by means of high resolution transmission electron microscopy (TEM). Summarizing the results of much literature data, one may

approximate the dependence of coercivity on particle size for maghemite nanoparticles by the curve shown in figure 1. Experimental data may be analytically approximated by

$$H_C(D) = H_M \cdot \left(\frac{D}{D_1}\right)^{-0.6} \cdot \left(1 - e^{\left(-\frac{D}{D_1}\right)^5}\right). \qquad (2)$$

D_1 is a material specific particle diameter characterizing the transition to superparamagnetism. The power law with exponent −0.6 appearing in this equation was found experimentally by Heider *et al* [94]. It describes the general increase of coercivity with decreasing particle size from multi-domain via various pseudo-single domain states (for instance the so-called vortex and flower states [219]) down to the single domain state. However, below a critical diameter (for example about 18 nm for maghemite) coercivity ceases due to superparamagnetic fluctuations. That rapid decrease is represented by the exponential term in the brackets of equation (2).

2.1.2. Magnetic relaxation. In principle, magnetic hysteresis is a non-equilibrium process. This means that after shutting off the external field, the macroscopic magnetization will tend to vanish with a typical relaxation time τ. Though this time is assumed to amount to millions of years in magnetic minerals —which is used by paläomagneticians to construct models of the Earth magnetic poles movements [55]—the relaxation times of small nanoparticles may vary down to very low values below that of seconds. The reason for this reversal of the magnetic moments in a magnetic material after vanishing of the aligning external magnetic field is the thermal agitation kT. For magnetic single domain nanoparticles the energy barrier against reversal of the magnetization is given by KV where K is the magnetic anisotropy and V is the particle volume. The relaxation time decreases rapidly with decreasing particle volume according to

$$\tau_N = \tau_0 \cdot e^{\frac{K \cdot V}{k \cdot T}} \quad \tau_0 \sim 10^{-9}\text{s}. \qquad (3)$$

This process is commonly called Néel relaxation [160]. It is the only relaxation process occurring in nanoparticles in MPH when being immobilized, as for instance in tumour tissue [63].

In comparison to the above, a further relaxation path may occur in fluid magnetic particle suspensions due to the ability of particles to rotate freely. Diluted suspensions called ferrofluids have found various technical applications [164]. For example, a common ferrofluid currently in use consists of magnetite (Fe_3O_4) or maghemite (γ-Fe_2O_3) suspended in organic carrier fluid. Aqueous carrier fluids are typically avoided in technical applications, because additional efforts to stabilize the particles by special coatings (see below) are required. In such fluid suspensions, the relatively high anisotropy barrier may be avoided by rotation of the whole particle under the influence of the external magnetic field. Instead of internal hysteresis loss, frictional losses due to *viscosity* η of the carrier liquid arise. The resulting relaxation

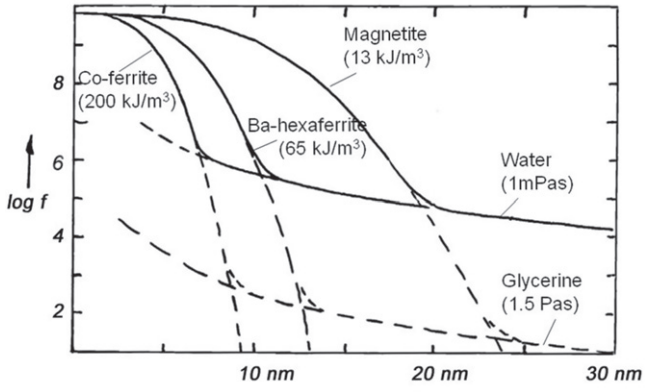

Figure 2. Relaxation frequency according to the Neél and Brown mechanism, respectively, in dependence on the particle diameter for different combinations of magnetic particle types and suspension media.

Table 1. Parameters d_C and f_C separating Brown and Néel spectral regions.

Ferrofluid type	d_C (nm)	f_C (kHz)
Maghemite/water	20	100
Maghemite/ester oil	24	0.1
Ba-hexaferrite/water	12	800
Co-ferrite/water	7	2000
Co-ferrite/glycerine	9	1
Co, hexag./water	6	4000

time is given by

$$\tau_B = \tau_0 \cdot \frac{3\eta \cdot V_h}{k \cdot T}, \qquad (4)$$

where V_h is the hydrodynamically effective volume, which may differ from the geometrical volume of the particle due to adhering fluid layers, for instance. The process is commonly termed *Brown relaxation* [31]. In literature one may find ambiguous opinions on the appearance of either Neél or Brown relaxation. Of course, particles will choose the energetically 'easiest way' for reversal of magnetization. This means that reversal will occur via that process which has the smaller relaxation time. In figure 2 the dependence of the relaxation frequency ($\sim 1/\tau$) on the particle size is shown for three types of nanoparticles only differing with respect to their magnetic anisotropy (data indicated in brackets in the figure), as well as two suspension media showing different viscosity (also given in the figure). All curves reflect clearly the different typical size dependences of Neél relaxation (equation (3) ~exponential) and Brown relaxation (equation (4) ~power law). Due to these very different mathematical laws one may easily decide, for any combination of particle types and suspension media, which relaxation mechanism is the predominant one for a particular pairing of particle size and external frequency choice.

The transition between both relaxation paths is given by $\tau_N = \tau_B$. It depends according to equations (3) and (4) on the particle volume, and figure 2 shows that for smaller diameters

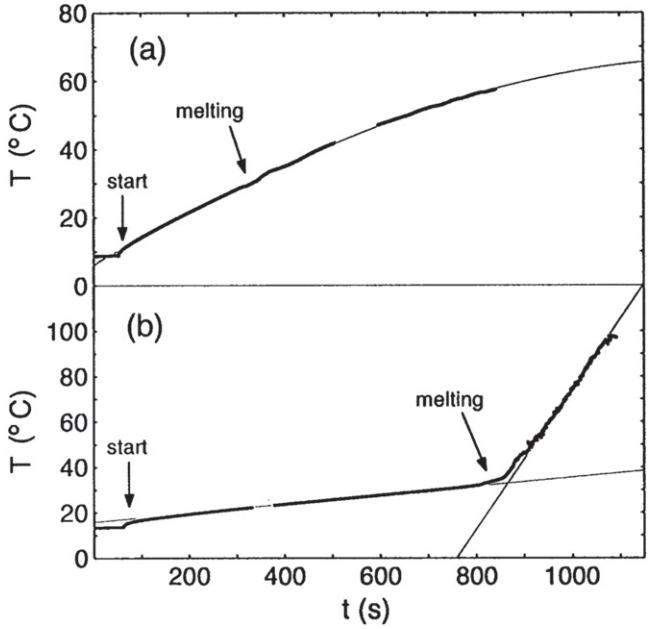

Figure 3. Temperature increase by magnetic heating of superparamagnetic (a) and ferrimagnetic (b) nanoparticles suspended in gel, from [102] with permission of Elsevier.

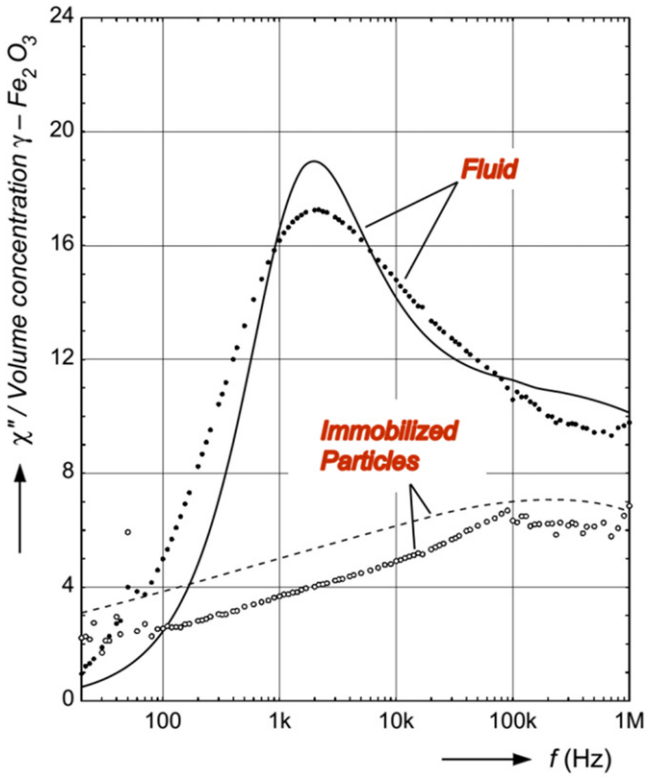

Figure 4. Calculated spectra (full lines) and experimental data (points) of the imaginary part of the specific susceptibility of a maghemite aqueous suspension in comparison to the same particles immobilized in gel, from [100] with permission of Elsevier.

Néel relaxation is more favourable than Brown relaxation. In table 1 the critical transition diameter (d_c) for both relaxation modes together with the corresponding relaxation frequency (f_c) is given for some practically interesting combinations of magnetic particles and suspension media (not only for hyperthermia).

The table shows that the appearance of a special relaxation path may vary considerably between different suspension systems. Moreover, it shows how crucially the actual relaxation path depends on the frequency of the applied alternating magnetic field. In particular, the strong effect of suspension viscosity is reflected in the typical frequency value f_C separating both relaxation regimes.

In figure 3 an example of heating curves of MNPs [102] is represented showing a kink which is a consequence of the existence of two relaxation paths. There, two iron oxide particle types differing mainly in mean diameter (8 nm (a) and 100 nm (b)) were suspended in gel which has a melting point at 30 °C. During heating by an alternating magnetic field of 410 kHz the appearance of Brownian losses in the case of the larger particles is clearly marked by a sudden temperature increase.

The Brown relaxation peak in the susceptibility spectrum of maghemite aqueous suspensions may be almost completely suppressed in favour of the Néel relaxation by immobilizing the particles in the gel, as demonstrated by the data shown in figure 4 [100]. In similar way, Brown relaxation is suppressed when particles are located in tumour tissue as shown by Dutz *et al* [63]. If magnetic particles are taken up by the tumour cells they are either locked in the cell plasma or adhere to the cell walls—as proved by various TEM investigations. Consequently, contrary to some discussions in literature, Brown relaxation is rarely an issue for hyperthermia as far as particles are applied by direct tumour injection. The use of fluid suspensions of magnetic particles in tumour therapy is dictated only by the need to apply the particles either by means of direct injection into the cancerous tissue or by transport in blood vessels guided by antibodies to the tumour. Accordingly, considering the heat output under a hyperthermia treatment one should differentiate whether particles are immobilized in tumour tissue or are freely movable in blood vessels. Insofar, one should be cautious to apply the heat output which is measured in liquid suspensions in laboratory conditions to real-life therapy planning, as is often done.

The full spectral curves shown in figure 4 were calculated by applying an often used model of magnetic relaxation. In this model linearity in terms of the applied magnetic field is supposed for the magnetization processes in alternating magnetic fields [186]. The magnetic susceptibility of the particle ensemble is taken to be independent of the external magnetic field H, which of course is approximately valid only for small field amplitudes. The corresponding problem of dipolar relaxation was treated firstly by Debye [45] for the case of electrical polarization of molecules. The principles discussed by Debye hold for magnetization relaxation, too. Consequently, one of his basic formulas is commonly used for the description of the frequency dependence of the imaginary part of the magnetic susceptibility χ''. For a relaxation process with characteristic time τ the susceptibility

χ'' is given by

$$\chi''(f) = \chi_0 \cdot \frac{2\pi \cdot f \cdot \tau}{1 + (2\pi \cdot f \cdot \tau)^2},$$
$$\text{with } \chi_0 = \mu_0 \cdot \frac{M_S{}^2 \cdot V}{a \cdot k \cdot T},$$
$$\text{and a} = 1\text{–}3. \quad (5)$$

The satisfying applicability of relaxation theory for small field amplitudes is shown by the data of figure 4 for aqueous suspensions of maghemite nanoparticles including both relaxation paths according to Néel and Brown.

If for small field amplitudes the susceptibility may be assumed to be independent of the field amplitude, one may calculate the frequency dependence of the loss power density according to

$$P(f, H) = \mu_0 \cdot \pi \cdot f \cdot H^2 \cdot \chi''(f) \left[\mathrm{Wm^{-3}}\right]. \quad (6)$$

See textbooks of electrodynamics, e.g. [133]. By using the mass density ρ of the magnetic material the SLP results:

$$SLP = \frac{P}{\rho}\left[\mathrm{W\ g^{-1}}\right]. \quad (7)$$

Unfortunately, the restrictions of the relaxation theory to small field amplitudes and small particle size are overlooked by some authors. In particular, the proportionality of losses with $f \cdot H^2$ often is used beyond the validity range of equation (6). The limitations of heating efficiency of small superparamagnetic particles, in the frame of the Néel relaxation model, in comparison with hysteresis losses in larger ferrimagnetic particles were shown by Hergt *et al* [96]. Later on, Rosensweig [186] applied the relaxation model for discussing the optimum particles size for superparamagnetic particles with respect to high SLP. The often overlooked validity limits of the Neél relaxation model were discussed by Hergt *et al* [99].

The example of experimental data shown in figure 4 demonstrates that ac-susceptibility is a valuable tool for checking the dependence of magnetic losses over a wide frequency range, at least for small field amplitudes. Alternatively, relaxation spectra may be measured in the time domain, too (e.g. [128]). This so-called magnetorelaxometry allows larger field amplitudes, but is restricted to smaller frequencies due to limited time resolution.

2.2. Magnetic field parameter choice

In the preceding section, we have shown that various modes of conversion of magnetic energy into heat may occur in MNPs. These modes differ principally in their dependence on the external parameters, the field amplitude and frequency. A major and controlling role is played by the mean particle diameter. The transition from multidomain to single domain magnetic behaviour occurs in a relatively broad size range at about 30 nm. In this transition region complicate spin structures as for instance the so-called vortex and flower states [219] may appear.

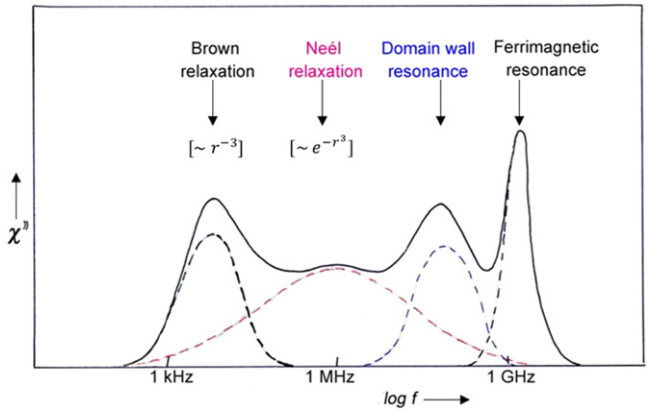

Figure 5. Frequency spectrum of the imaginary part of susceptibility of magnetic nanoparticles for small field amplitude (schematical).

2.2.1. Field frequency. With decreasing particle size the influence of thermal fluctuations increases rapidly. The particles show superparamagnetism, which is observed if the changes of the external field are too slow in comparison to the relaxation time. Insofar, the transition from stable ferromagnetic to superparamagnetic behaviour depends on the frequency of the external field. Furthermore, it depends on particle size according to equations (3) and (4). The transition range is, in the particular case of the exponential dependence of the Néel relaxation, rather sharp. For magnetite with an effective anisotropy energy density of 10 kJ m^{-3} the critical size at 400 kHz is about 18 nm [99].

The appearance of superparamagnetic fluctuations is of importance in choosing the suitable frequency in relation to the particle diameter. In general, at low frequency the magnetization M of a particle ensemble may easily follow the driving alternating magnetic field H, i.e. M and H are in phase. With increasing frequency, however, M cannot follow the rapid changes of H. A phase lag appears, which results in the susceptibility becoming a complex number. Its imaginary part describes losses according to equations (5), (6). A recent survey on relaxation effects was given by Coffey and Calmykov [41]. A comprehensive theory of the dynamic susceptibility of magnetic fluids was presented by Shliomis and Stepanov [196], even including the effect of particle size distributions. All of these authors deal with the complete susceptibility spectrum. In addition to the relaxation peaks (of Debye type) they also take into consideration the resonance peak (of Lorentz type) of the so-called ferromagnetic resonance. In figure 5 the different possible contributions over the whole spectrum of the imaginary part of the magnetic susceptibility are shown schematically. Besides the Brown and Néel dispersion regions mentioned above, in multidomain materials, at high frequencies, a loss peak due to domain wall resonance may be observed. At microwave frequencies the ferrimagnetic resonance of the spin system appears.

The application of microwaves in tumour therapy is known, as already mentioned in the introduction. However, the combination with MPH is questionable since technically achievable field amplitudes in the microwave region are rather small. Insofar, one should be cautious in extrapolating related

experimental findings from small *in vitro* cell cultures to MPH therapy. However, this issue may deserve further elucidation under consideration of technical, but also safety-related boundary conditions.

At low frequencies in the superparamagnetic regime ($f\tau \ll 1$) the power increases with the square of frequency according to the combination of the equations (5) and (6). At frequencies above the relaxation maximum ($f\tau \gg 1$) these equations predict the losses to saturate at $P = \mu_0 \pi H^2 \chi_0 / \tau$ independent of frequency. However, when $f\tau \gg 1$, one has already left the superparamagnetic regime and the predictions of the Neél relaxation model become obsolete.

Besides an increase of the field frequency, a large value of the field amplitude is also attractive for hyperthermia, since the heating power given by equations (5)–(7) is proportional to H^2. However, following that trend one quickly exceeds the range of validity of the simple linear model, too. Many authors overlook the limiting suppositions of the Neél relaxation model when extrapolating SLP by means of the fH^2-term of equation (6). In particular, thermal energy kT must be larger than magnetic energy μ_0MHV—a condition which ceases for large field amplitude. Accordingly, the valid region of the Néel relaxation model is very restricted considering MPH: First, a rise of frequency may lead out of the regime of superparamagnetism and, second, an increase of field amplitude leads out of the validity range of linear approximation. Consequently, to achieve large heating power one has to leave the Néel relaxation model and to take into consideration larger, ferrimagnetic single domain particles [99].

2.2.2. Field amplitude. Unfortunately, leaving the small linear region of field amplitudes leads to mathematical complications arising with the description of the nonlinear hysteresis loop (see e.g. [24]). To overcome these difficulties a semi-empirical approach was presented by Hergt *et al* [98]. Using the size dependence of coercivity $H_c(D)$ given in equation (2), the specific energy loss per hysteresis cycle may be described by

$$\mathrm{SHL}(H, D) = \begin{cases} \alpha \cdot D \cdot H^3 & \text{for } H \leqslant H_C \\ \dfrac{4B_R \cdot H_C(D)}{\rho} \cdot \left(1 - \left(\dfrac{H_c(D)}{H}\right)^5\right) & \text{for } H > H_C \end{cases}. \quad (8)$$

For field amplitudes below the coercivity H_c a Rayleigh term proportional to H^3 is taken into account, since many experiments of the present authors have shown such friction-like behaviour of domain walls, even in the so-called 'single-domain' size range [56, 61]. Equation (8) shows, that the model is based only on three material parameters: coercivity H_c, remanence $B_R = \mu_o M_R$ and the 'friction parameter' α. These parameters may vary in a characteristic way for particles prepared by different methods. Equation (8) offers the opportunity to check the heating efficiency of MNPs in a diameter-amplitude-diagram which is shown in figure 6. In a three dimensional (3D)-plot the hysteresis loss is plotted in

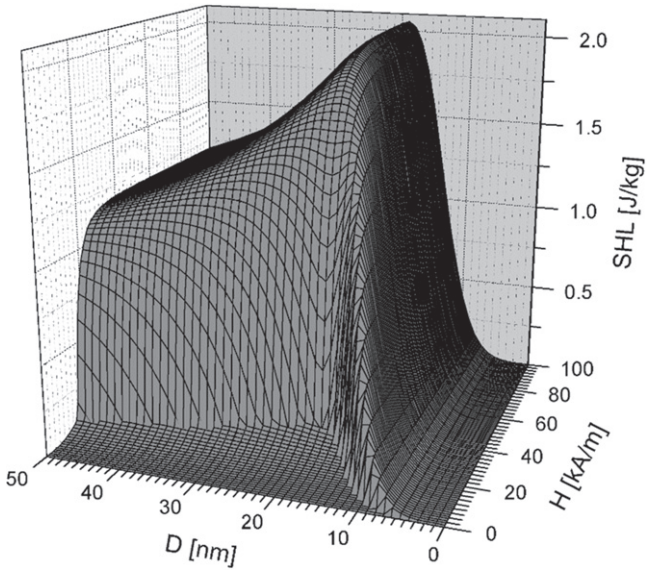

Figure 6. Dependence of specific hysteresis losses per cycle on mean particle diameter D and magnetic field amplitude H for monodisperse maghemite nanoparticles, from [98] © IOP Publishing. Reproduced by permission of IOP Publishing. All rights reserved.

dependence on both, particle size and field amplitude for monodisperse maghemite nanoparticles. Parameters are the values of coercivity and critical particle size of figure 1.

For small particle diameters the figure shows the steep slope of the loss dependence in the superparamagnetic regime. Above the transition from superparamagnetic to single-domain behaviour the maximum of loss energy per cycle appears. For small field amplitudes the loss is negligibly small, too, until the amplitude is increased above the coercivity field H_c. Above about 30 kA m^{-1} useful loss saturates. This makes a further increase of field amplitude beyond that value unreasonable. At larger particle size the transition to the multidomain range occurs and loss energy again becomes smaller.

Taking into account that the SLP is given by the product of SHL multiplied by the frequency, the 3D diameter-amplitude-diagram may be used for choosing the most favourable amplitude–frequency pairing. This choice has to be tailored to the available particle sort. Moreover, it has to fulfil many medical restrictions and technical or economical conditions regarding the therapeutic apparatus. For a field maximum of 30 kA m^{-1}, the eddy current limit for patient health, to be discussed below, would allow a maximum frequency of 150 kHz which results in an SLP of about 300 W g^{-1} in the present case.

While the Stoner–Wohlfarth-model predicts complete vanishing of loss below H_c, the present model shows a typical low loss region which resembles the losses due to wall displacement in multidomain particles. However, in the diameter range just described, typical domain walls do not exist. Instead, the already mentioned flower or vortex states of spin structure may appear. Unfortunately, until now nothing is known on the dynamic behaviour of those complicated structures, in particular with regard to magnetic losses.

However, those low field losses are typically observed for nanoparticles prepared in very different way [56, 61]. It was shown [98] that these results may be explained by size distributions. The correlation between particle size and the resulting reversal losses as shown in figure 6 was confirmed experimentally by means of quasistatic measurement of hysteresis curves [61, 96, 116] as well as by thermal measurements [8, 16, 44, 71, 123, 126, 157].

In general, nanoparticle ensembles show a size distribution. The incorporation of the size distribution in the equations determining the diameter-amplitude-diagram [98] offers interesting practical conclusions for MPH to be discussed in section 4.2. Moreover, technical field parameters must be carefully chosen in order to fit well with particle properties. The latter one may vary appreciably in dependence on preparation conditions as will be shown in the next section.

3. Preparation of MNPs

According to the above discussion, the magnetic properties of nanoparticles depend on their structural and morphological properties. Strong variations of the structural properties and morphology were found for particle samples of comparable size but preparation by different routes. The most common routes are wet chemical methods, but there are many other methods including laser evaporation, milling of larger particles, or biomineralization in bacteria. Thus, the resulting SHP of MNP may vary substantially depending on preparation conditions during different preparation routes. The following section provides a short introduction to the main iron oxide MNPs preparation routes. Detailed information can be found in excellent reviews on this topic [17, 140, 204], and the current state of the art is given by Hasany *et al* [92] and Grüttner *et al* [84].

3.1. Preparation of magnetic cores

3.1.1. Liquid phase synthesis. This synthesis route is a well-established and relatively simple method for preparation of larger amounts of MNP. Generally, the liquid growth medium may be any organic phase, but most scientific work deals with precipitation in aqueous media. Typically, magnetic iron oxides (maghemite or magnetite) are prepared by means of co-precipitation from aqueous Fe^{2+} and Fe^{3+} salt solutions by addition of a base. Magnetic phase and particle size can be controlled mainly by variation of iron salts, Fe^{2+}/Fe^{3+} ratio, temperature, pH, and type of base. Fundamental work on this preparation route was done by Khallafalla and Reimers [125] and Massart [150]. Typically, particles are in the superparamagnetic size range from 5 to 15 nm and size distribution is relatively broad. By changing reaction conditions size can be increased up to 40 nm [61], where particles show single domain ferrimagnetic behaviour. Different modifications of this method have been reported in recent years. For a smaller size distribution, particle nucleation must be prevented during particle ripening which can be realized by a cyclic growing process [156]. A high pressure homogenization during precipitation [85] or decelerated reaction conditions [56, 57] resulted in clusters of single crystals of 15–20 nm which show high SHL and thus making them interesting for hyperthermia [63, 110, 137].

Another important aqueous liquid phase preparation route is based on the oxidative alkaline hydrolysis of Fe^{2+} solution [9, 62]. Fe^{2+} salt ($FeSO_4$ or $FeCl_2$) is dissolved in distilled water, then an alkaline medium (NaOH or KOH) and an oxidizing agent (KNO_3) solutions is added drop-wise. By using this method, the resulting particle size may reach 100 nm, whereby the large ones already show multi domain behaviour [61]. Li *et al* [143] investigated effect of initial $Fe^{2+}/NO_3^-/OH^-$ ratio on size, morphology, and heating power and found maximum SHP for 36 nm maghemite particles.

3.1.2. Polyols synthesis. Polyols synthesis, based on the oxidative alkaline hydrolysis of Fe^{2+} and Fe^{3+} salts in a mixture of polyols (e.g. polyethylene/diethylene glycol or *N*-methyldiethanolamine). MNP from polyols synthesis show interesting heating behaviour, despite the particles not being monosized. Their interesting behaviour is caused by their special morphologic structure. By choice of temperature, type of solvents, and reaction velocity the size and structure of resulting MNP can be controlled [110]. Under certain reaction conditions, so called flower-shaped MNP can be prepared by this route [110] which show SHP of up to 2000 W g^{-1} [137]. Actually, these particles are multicore nanoparticles consisting of single cores of about 8–10 nm which form clusters of about 30 nm and have been found to be very interesting for hyperthermia before [57].

3.1.3. Thermal decomposition synthesis. A further promising way for MNP preparation is thermal decomposition of organometallic compounds (precursors) in high boiling organic solvents. The main advantage of such particles is a very narrow size distribution. Typically, iron carbonyls or iron acetylacetonates are used as precursors and oleic acid or fatty acid serve as surfactants. Size and morphology of resulting particles is controlled by ratio of precursors to starting agents (surfactants and solvents). Actually, thermal decomposition of carbonyl precursors leads to pure iron (metal) but in a second step these metal particles are oxidized to iron oxide by moderate heating under mild oxidative conditions. A one-step route to prepare iron oxide particles is thermal decomposition of precursors with cationic iron centres (e.g. $Fe(acac)_3$). Fundamental work in thermal decomposition preparation was done by Hyeon *et al* [112] and Park *et al* [173] who prepared nearly monosized particles of about 13 nm. Several groups modified the method of Hyeon and Park and obtained MNP in the size range from 5 to 18 nm with SHP promising for hyperthermia [81, 126, 142].

3.1.4. Hydrothermal reactions. Hydrothermal reactions are performed in aqueous media at temperature above 200 °C realized in autoclaves at pressures of 2000 psi and more. Such

reactions base on the ability of water to hydrolyze and dehydrate metal salts at high temperatures and the low solubility of obtained metal oxide particles in water at such temperatures [90]. Particles size and morphology is mainly controlled by concentration, temperature, and autoclaving time [222]. Typical sizes are in the range from 10 to 50 nm. Size and distribution width of the particles are mainly determined by autoclaving time and increases with duration of autoclaving. For short autoclaving times monosized particles can be obtained [169, 222].

3.1.5. Microemulsion synthesis. In micro-emulsion synthesis, a two-phase method is used to produce near mono-sized distribution. For this, nanosized water droplets (10–50 nm) are dispersed in an oil phase (water-in-oil microemulsion) and stabilized by surfactant molecules at the water/oil interface [6, 42, 134]. These droplets serve as micro reaction vessels which limit diffusion distance and thus nucleation, growth, and agglomeration of particles and thus results in more uniform particles [174]. Particles from microemulsion synthesis show a high binding affinity to biological material [166] and an SHP suitable for hyperthermia [230] making them especially interesting for medical applications.

3.1.6. Laser evaporation synthesis. A suitable method for preparation of large amounts of MNP powders is laser evaporation. The initial materials are coarse haematite powders of a few μm particles [130, 131], metallic micropowders or massive iron blocks, respectively [154]. The starting material is evaporated by means of a laser within an evaporation chamber. Due to the relatively steep temperature gradient outside of the evaporation zone a very fast condensation of fine particles takes place from the gas phase. The condensed particles are removed from the evaporation/condensation zone by airflow and are deposited on a filter made of paper or metal. The resulting product is a fine powder of maghemite/magnetite with a low tendency to form agglomerates and a relatively narrow size distribution. Resulting mean particle size (20–50 nm) and magnetic phase are controlled by laser power and composition of atmosphere in evaporation chamber [201].

3.1.7. Biomineralization. Magnetotactic bacteria are capable of synthesizing magnetosomes (the core of which consist of nanosized crystals of magnetic iron oxide), serving as a compass to find their preferred habitat on the bottom of the sea [20]. Under well-defined synthesis conditions in the lab, which reproduce the anaerobe condition of their habitat, uniform particles of 20–45 nm core diameter may be produced [192, 193].

During biomineralization Fe^{2+} and Fe^{3+} ions are incorporated by the bacteria from the surrounding media and transported to a vesicle already formed in the bacteria [19]. Ions of Fe are then oxidized to Fe^{3+} oxide within the vesicle, which reacts with the Fe^{2+} ions and form Fe_3O_4. These particles can be extracted from bacteria by means of cell disruption. Despite magnetosomes displaying an excellent SHP of about 1000 W g^{-1} at relatively low magnetic field amplitude [101, 212] they have currently found no use in medical applications, because their coating consists of bacterial proteins. Recent research on magnetosomes aims on elucidation and optimization of the biomineralization process [18, 191] and to transfer these findings in wet chemical preparation routines, thus providing MNP with similar magnetic behaviour as magnetosomes.

3.1.8. Sol–Gel method. Sol–gel method allows synthesis of a variety of metal oxide particles/structures and is very easy to perform [95, 161]. Synthesis is based on hydroxylation and condensation of precursors in solution (sol) containing metal ions. After gelation of the 'sol' by solvent removal or chemical reaction, a 3D metal oxide network is obtained in the 'gel'. A drawback of this method is the dominating synthesis of nanostructured networks rather than single MNPs of defined size.

Other preparation routes for MNPs, which will not be treated here in this article since the resulting particles are not of high relevance for medical applications, are *Glass Crystallization*, *Spray and Laser Pyrolysis*, *Sonolysis*, and *Microwave Irradiation Synthesis*.

3.2. Coating of magnetic cores

In most cases for medical application of MNPs, the particles must be transformed into a ferrofluid which requires a coating of the magnetic cores by a specific layer. There are several reasons for the necessity of such a layer:

- Prevention of agglomeration and sedimentation of the MNP within a ferrofluid (stabilization).
- Warranty of biocompatibility of the ferrofluid.
- Coupling of different features on particles surface by means of a coating serving as an anchor layer (functionalization).

3.2.1. Stabilization. When using ferrofluids for medical applications the fluids must resist agglomeration and sedimentation. Usually, for small superparamagnetic MNP van-der-Waals forces lead to agglomeration of MNP and for larger remnant ferrimagnetic particles magnetic attraction between single particles is responsible for agglomeration. When agglomerates exceed the critical sedimentation size, the agglomerates form sediment, in which very large particle clusters may occur. Such large aggregates in the ferrofluid might cause occlusion of a vessel leading to embolization of healthy tissue, or in the worst cases to myocardial infarction and apoplectic stroke which both carry enormous risk for patients. The critical sedimentation size (d_{crit}) is defined by:

$$d_{\mathrm{crit}} = \sqrt[3]{\frac{6 \cdot k \cdot T}{\pi \cdot \Delta\rho \cdot g \cdot h}}, \tag{9}$$

where k is the Boltzmann constant, T the temperature, $\Delta\rho$ the

density difference between particle and suspension media, g the gravity acceleration, and h the height of the sample.

Coating of the remnant magnetic cores with an uncharged material leads to an increase of the distance between single cores, which causes a decrease in the attractive magnetic forces and results in a so called *steric stabilization*. These particles show no interaction with other particles and are in permanent movement due to Brownian motion. In this case thermal energy is dominating the ever present gravitational energy and the fluid is homogeneously suspended. Typical coating materials for steric stabilization are dextran or starch.

In the case where steric stabilization is insufficient for stable suspension of particles (e.g. for large magnetic cores showing strong magnetic attraction forces) a stronger stabilizing effect can be obtained by means of *electrostatic stabilization*. For this, the particles are coated with a charged material resulting in a zeta potential of the particles of at least 30 mV (positive or negative) leading to strong electrostatic repulsion forces between the coated single cores. A typical coating material for such electrostatic stabilization is citric acid.

For practical reasons, often both effects are combined for so called *electro-steric stabilization*. A thick layer on the particle surface can produce a potential of more than ±40 mV and can be achieved by coating with polysaccharides bearing functional groups, e.g. carboxymethyl dextran, amino dextran, or chitosan.

3.2.2. Biocompatibility. Despite the biocompatibility [218] of iron oxide itself, depending on the preparation route, MNP may have surface modifications which result in toxic behaviour and thus prove to be unfavourable for medical application. Biocompatibility of such particles can be increased considerably by coating the core with a dense biocompatible layer which masks the toxicity of the core. Furthermore, charge and hydrophilic/hydrophobic behaviour of particles surface is very important for the biological fate of MNP [109]. Cellular uptake of positively charged MNP is very strong [220], but such particles usually show higher toxicity compared to negatively charged MNP—probably due to their high affinity to negatively charged cell membranes. Schweiger *et al* [194] found that negatively charged MNP were incorporated first into endosomes and later into lysosomes, whereas positively charged particles end up solely in lysosomes.

Therefore, by modification of particles surface chemistry and charge the biological behaviour of the particles can be controlled. This is confirmed by the latest investigations into the formation of a protein corona on the MNP surface when bringing them into a biological system. The composition of the protein corona formed by biomolecules from the biological matrix may vary [146, 148, 207] depending on particle size, surface area and morphology of MNPs as well as on the local environmental conditions. Laurent *et al* [139] found a clear correlation between composition of protein corona and cellular uptake and toxicity of particles. Investigation of protein corona formed during cellular uptake and the resulting biological fate of the incorporated MNP is a novel promising research field, which may lead to new and fundamental findings useful for the development of biocompatible MNP.

3.2.3. Functionalization. Another reason for particle coating is the possibility of coupling different features onto a particle's surface where the coating serves as anchor layer. A possible feature is the labelling of particles with a fluorescent dye. This enables the tracking of cellular uptake or biodistribution by means of optical detection [69, 162]. By using a pH dependent dye these particles can serve as nanoprobes for intracellular pH measurements [135, 136, 167]. Furthermore, the coating may serve for coupling drugs to the particles which can be enriched magnetically in the target region and enable a targeted drug delivery, after the release of the drug from the nanoparticles [3, 115, 145].

A most interesting feature for hyperthermia on particle surface is the conjugation to target specific bioactive molecules. Functionalization of a particle's surface with monoclonal antibodies, antibody fragments, or other target specific biomolecules [12] enables a targeting of MNPs directly to the tissue or object of interest. The particles find their target automatically after systemic application and an accumulation of particles in the target region occurs. In this way, the magnetic labelling of tumours for hyperthermia applications can be achieved—up to now with relatively low particles concentration within tumours only, which are not sufficient for therapeutically suitable hyperthermia [114, 213]. Many ways to couple such molecules to the particles surface are described in literature [84, 152, 216].

3.3. Size dependent fractionation

Commonly the preparation of monosized particles is very challenging. Another possible way to obtain particles of exactly one size or at least particles with narrow size distribution is size dependent fractionation of particle ensembles with a rather broad size distribution. For this, particles of the desired size are extracted from the original sample or particles above and below a defined threshold are removed from the sample to obtain particles of certain size. Insofar, size dependent fractionation leads to narrowing of size distribution resulting in notable increase of heating power in specific fractions [57, 77] which will be discussed in more detail in the next section.

Typically, particle ensembles are split by means of gravitational forces and centrifugation [23, 57], magnetic forces [39, 73, 77, 211, 229], or changing the repulsion forces between single particles by varying the zeta potential of the particles, which is controlled by means of a variation of the pH of the sample [37].

All of these methods suffer from the problem that they are only suitable for batch processing of limited sample volumes. The implication is that the quantity of fractionated material produced per batch is relatively low and thus these

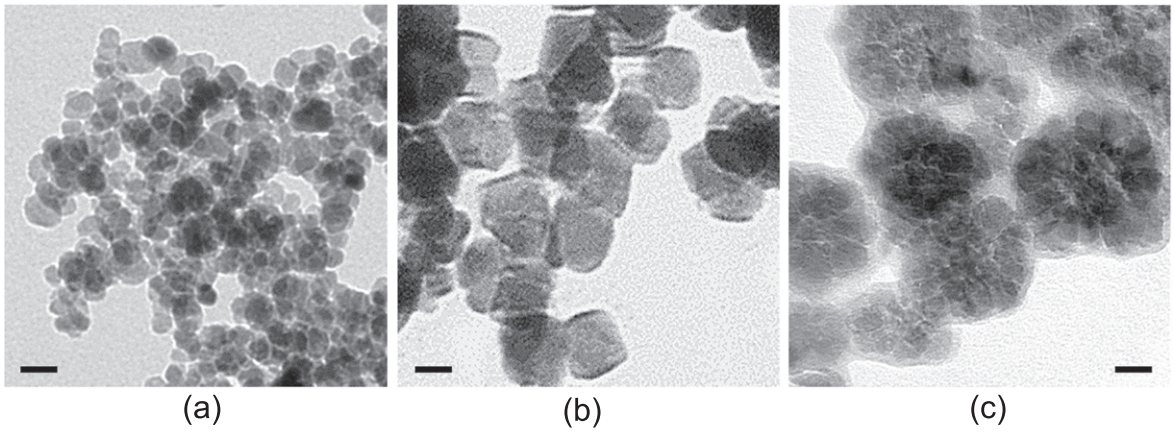

Figure 7 TEM of different particle types: small superparamagnetic single domain particles (a), larger ferrimagnetic single domain particles (b), and superferrimagnetic multicore particles (c), size bar 20 nm.

methods tend to be suitable only for the processing of analytical quantities.

To overcome this drawback, several microfluidic methods for continuous fractionation of nano/micro-particles have been developed. The majority of them use filtration [159, 224], gravity forces [111], sound pressure [138], optical forces [153], magnetic forces [34, 171, 197, 228] or fluidic forces [25, 58, 198] for the classification of magnetic particles. Comprehensive reviews about recent developments in this field are given by Pamme [170] and Adams [1].

Inspite of the relatively low reproducibility of some techniques size dependent fractionation is a valuable tool to investigate size effects in magnetic heating. The most reproducible commercially available fractionation method is asymmetric flow field-flow fractionation [64, 144].

4. Structure of MNPs

4.1. Structural investigation

As described in section 3.1 particle preparation following different routes results in a strong variation of particles size, size distribution, and also particle morphology. These structural and morphological properties are mainly responsible for resulting magnetic properties of the prepared particles. In the opinion of some people MNPs are ideal spheres on the nanometre scale, which is not appropriate in most cases. Figure 7 provides representative examples for different particle morphologies.

As can be seen from figure 7, particles of spherical shape are the exception and in fact almost any particle morphology can conceivably be made, e.g. cubes, needles, triangle, multicores, irregular shapes, and much more. Since particle size and shape determines crystal and shape anisotropy and thus the ever important coercivity, it is very important for development of suitable hyperthermia absorbers to control these parameters. This requires a thorough and rigorous characterization of the prepared particles.

The most common method to evaluate structural properties of MNPs is TEM. This technique enables a direct visual view of the particles and provides a good impression of particle shape. However, one should keep in mind that resulting images are overlaps of several object planes. This can lead to misinterpretation of particle shape when looking at single particles without sufficient statistical certainty, e.g. a single needle can look like a sphere when looking just on the front side. Beside the information on particle shape TEM provides also a mean diameter and polydispersity index by means of statistical evaluation of larger amounts of imaged particles. When using high resolution TEM, atomic planes can be displayed which gives information about crystal structure of particles.

A more prevalent technique for investigation of crystal structure of particles is x-ray diffraction (XRD). With this method the unit cell, atomic planes, lattice constant and other crystal parameters can be determined which enables a reliable detection of magnetic phase and lattice structure of particles. From the broadening of the diffraction pattern, the mean volume of coherent scattering areas in the particles can be estimated by means of Scherrer formula. This provides the particle size for single crystalline particles or the size of single cores of multicore particles. Mean particles size is the most influential factor on the magnetic properties of more or less spherically shaped MNPs, as described in section 2.

The determination of overall core particle size can also be done by means of atomic/magnetic force microscopy, small-angle neutron scattering or small-angle x-ray scattering but in most cases combination of TEM and XRD gives the most reliable information about particle size, size distribution, morphology, and inner structure of prepared particles.

4.2. Particle size distribution effects

As discussed in the previous sections, for particles of exactly one size (monodisperse), the dependency of magnetic properties on structural properties can be described reliable by theory and on the basis of empirical findings (cf figure 6). However, the preparation of monodisperse particle ensembles

is very challenging and thus for real particles the polydispersity of particle diameters must be taken into account. This polydispersity of particle sizes can be described as a log-normal distribution:

$$f(D) = \frac{1}{\sqrt{2\pi} \cdot \sigma \cdot D} \exp\left(\frac{-\left(\ln D/D_0\right)^2}{2\sigma^2}\right), \tag{10}$$

where D_0 is the median and σ the standard deviation of ln$D$. The mean diameter is given by

$$D_m = D_0 \exp\left(\frac{\sigma^2}{2}\right), \tag{11}$$

and the volumetric heating power of the polydispersion $\overline{P}$ can be obtained by numerical integration over the distribution function:

$$\overline{P} = \int_0^\infty P \cdot f(D) \cdot \mathrm{d}D. \tag{12}$$

For numerical calculations of reversal losses, taking into account size distributions for particle ensembles, the Γ-distribution can be used instead of the log-normal distribution which is equivalent in shape but has advantages for the numerical calculation of the integrals [2].

In several simulation studies of different groups (e.g. [81, 186]), it was found that samples with the narrowest size distribution yield the highest reversal losses. All the presented simulations and investigations were restricted to a relatively narrow size range of superparamagnetic particles and considered only the existence of one mechanism (relaxation) during reversal of magnetization. However, due to the size distribution of real existing particle ensembles, a proportion of superparamagnetic, ferrimagnetic and as well as even a (small) proportion of larger multi domain particles should be taken into account. This may be performed on the basis of the semi-empirical model described in section 2.2. In the framework of that model, magnetic losses were calculated taking into account the size distribution [98]. Calculations of the losses of a polydispersive system were carried out by numerical integration (equation 12) of the reversal losses as a function of field and mean diameter (equation 8) over the distribution function (equation 10). In figure 8 the dependence of losses on the mean particle diameter is compared for a small (diagram (a)) and a broad (diagram (b)) size distribution. The effect of field amplitude is included in the figure as a parameter.

As expected, the broader distribution of particle size has a moderate effect on the size dependence of losses. Contrastingly, the narrow distribution group shows a marked depression of losses for medium mean sizes. A minimum of hysteresis losses is pronounced for lower field amplitudes. Reasonably, the curves of figure 8 represent sections at constant field amplitude through the 3D face shown in figure 6, which for broader size distribution become smoother. The maximum loss may be gained only if the field amplitude is well above the coercivity for the majority of particles. In fact, in a narrow distribution, loss is more sensitive with respect to the optimum choice of particle mean size while in a broader distribution this choice is not so critical. For optimum heat output with a narrow size distribution, particle properties and magnetic field amplitude must be carefully adjusted with respect to the particle properties. If this is not the case, e.g. if the field amplitude does not reach saturation, a broader size distribution may be favourable to get a acceptable heat output.

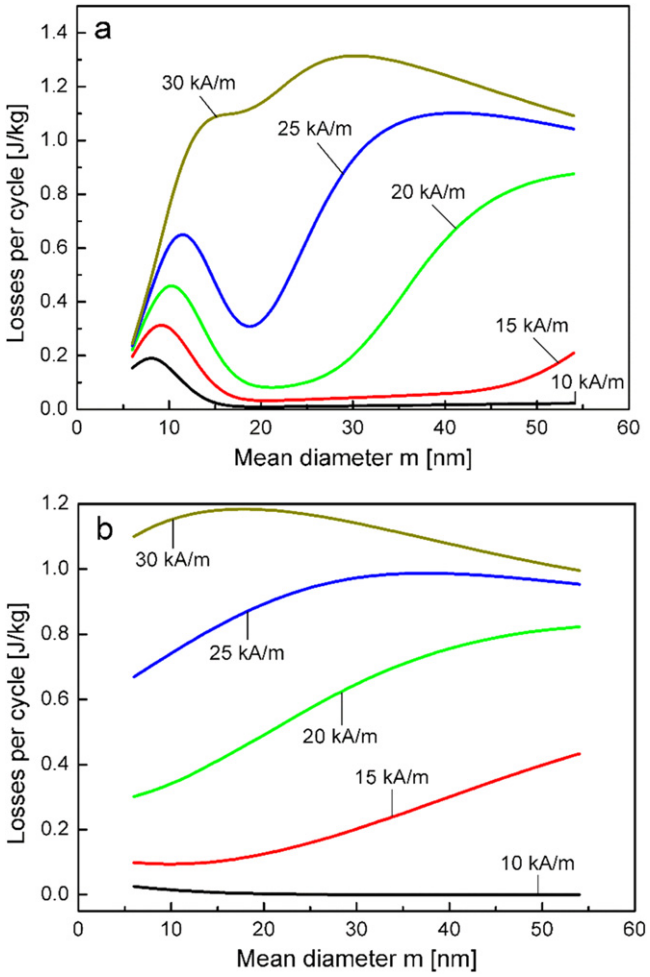

Figure 8. Influence of small (a) and broad (b) size distribution on magnetic losses for different field amplitudes, from [98] © IOP Publishing. Reproduced by permission of IOP Publishing. All rights reserved.

In addition to the effect of size on magnetic coercivity, other magnetic properties (e.g. saturation magnetization and remanence) depend on the size, shape, structure and chemical composition of the particles. These in turn influence the reversal losses that may occur. For instance, a dependence of magnetization on particle size [16, 158] or coating materials [227] or an influence of surface-to-volume ratio (size) of the particles on their anisotropy [72, 187] have been investigated.

4.3. Particle–particle interaction effects

Ferrofluids can be regarded as a non-magnetic matrix containing MNPs in different concentrations, which may be described as varying packing density of the particles. In literature, ferrofluids are often treated as coated magnetic single

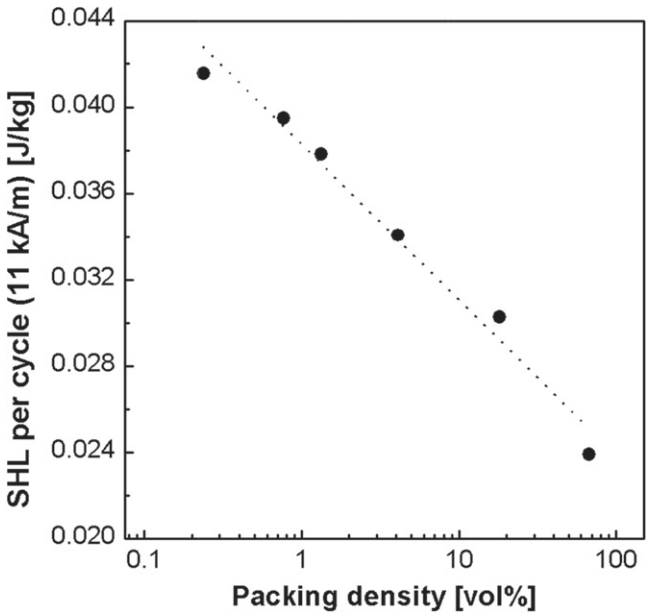

Figure 9. Dependence of the mass weighted specific hysteresis losses (SHL) on the packing density of magnetic nanoparticles measured at low field amplitude (11 kA m^{-1}), from [59] with permission of Sumy State University.

cores homogeneously dispersed in a carrier medium showing a constant distance between single cores. In reality this is not the case, as agglomeration of the single cores takes place due to magnetic attraction or van-der-Waals forces. Chantrell [38] showed, by Monte-Carlo simulations, that dipolar chains and flux closure configurations might form in a magnetic particle system of higher concentrations. The formation of dimers, trimers and larger aggregates due to dipolar interaction in stable ferrofluids was computed by means of Monte-Carlo simulation by Castro *et al* [35]. They found that at about 1% volume fraction a relatively small amount of agglomeration occurs and these are essentially dimers. Above about 10% volume fraction more than half of the particles are bound in agglomerations larger than trimers. The chain formation for relatively large particles (about 30 nm diameter) is well known from magnetotactic bacteria synthesizing fine magnetite crystals [54]. Of course, the tendency for agglomeration increases considerably with the transition from superparamagnetic to stable ferromagnetic single domain.

In simulations of the quasistatic remagnetization processes by various different numerical methods [22] a dependency of magnetic properties on packing density was predicted. There, the transition from single particle to collective behaviour with increasing volume concentration is discussed as a function of the particle magnetic anisotropy.

In experimental investigations [59, 195, 214], the alteration of magnetic properties by changing the packing density of ferrimagnetic particles was confirmed. Urtizberea *et al* [214] described an increase in heating power of about 100% when the concentration was decreased by a factor of 4. Dutz and Hergt [59] found a decrease of hysteresis losses down to 50% when changing packing density from 0.24% up to 67.6% (figure 9). In that study the ferrimagnetic stable particles ($D = 21$ nm) were dispersed and immobilized in a non-magnetic SiO_2 particles matrix in different particle volume concentration. It has to be pointed out that magnetization loops of solidified particle systems (e.g. powders) essentially differ from those of particles in liquid suspension. Most practical interest in magnetic particles refers to nearly immobilized particles [63, 180]. A dependency of coercivity, remanence and reversal losses on packing density was found, the highest values of these parameters appearing for samples with lowest packing density.

The observed decrease of coercivity, remanence and hysteresis losses with an increase of packing density may be related to increasing dipole–dipole interactions which disturb the energy landscape of the particle system by occurrence of local energy minima [66]. In contrast, a different behaviour can be supposed for superparamagnetic particles which show weak dipole interactions. Similar to ferrimagnetic particles, for the case of higher concentrations a stronger tendency to form agglomerates can be observed. Due to the dominating exchange interactions, the agglomerates behave like a particle with an effective volume larger than the single core and shows ferromagnetic behaviour with hysteresis. This agglomeration hypothesis is supported by experimental studies where increased coercivity and heating power were found for agglomerated superparamagnetic nanoparticles in comparison to single cores [48, 67, 226].

A special particle type with a behaviour which can be described neither by superparamagnetic nor ferrimagnetic theory in the classical sense are the so called multicore nanoparticles. These particles consist of a number of superparamagnetic cores of around 10 nm diameter which form clusters a few tens of nanometres large [56, 57]. The overall behaviour of these particles is ferrimagnetic, but coercivity and remanence are significantly lower than for single core particles of comparable size. Surprisingly, the heating losses are higher for multicore nanoparticles than for single core particles of comparable coercivity. Their special magnetic behaviour makes such particles very interesting for hyperthermia [63, 137] and other medical applications (e.g., magnetic particle imaging (MPI) [65]) despite the fact that their remagnetization behaviour is not completely understood [189, 190].

5. Damaging of the tumour

5.1. Heat transfer in tumour tissue

The magnetic energy supplied by the external alternating magnetic field to the MNPs is converted into heat within the crystal lattice of the nanoparticles. It caused some controversy in literature on which way this heat is delivered to the tumour tissue. Of course, the most probable mechanism of delivering heat to the surrounding medium is due to heat conduction. During field application a balance between heat generation in the particles and the flow of heat into the surrounding tissue must be established. It is this balance which determines the attainable temperature in the particle-containing tissue. Of

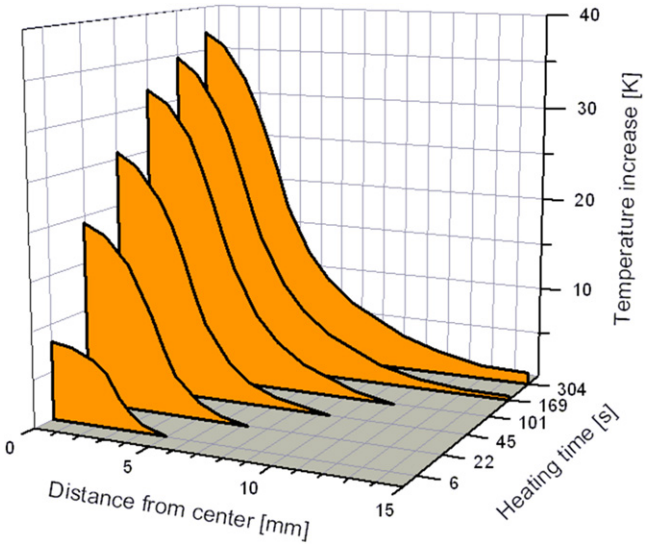

Figure 10. Temporal evolution of the temperature distribution around a spherical region of heat generation (radius 3.15 mm) calculated by solving the heat conduction problem, from [60] with permission of Informa Healthcare.

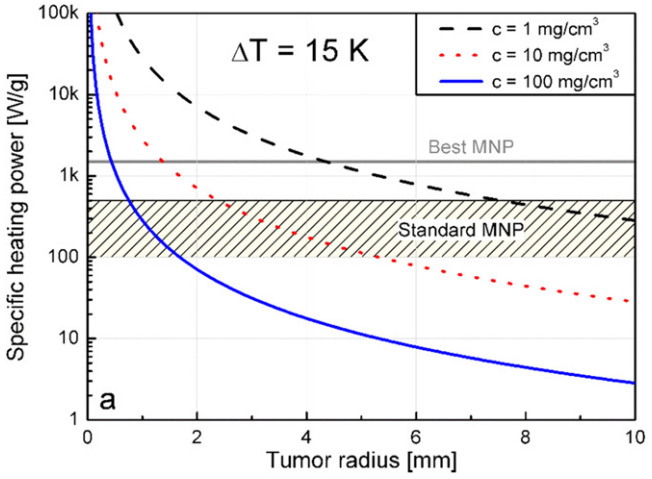

Figure 11. Demand of specific heating power (SHP) in dependence on tumour size for generating a temperature increase of 15 K with different MNP concentrations in the tumour tissue, from [60] with permission of Informa Healthcare.

course, the heat distribution depends on the distribution of particles located in the cell plasma or in the interstitial volume between tumour cells. Unfortunately, the particle containing tissue is very inhomogeneous, (e.g., cell membranes, varying cell size, cell shape and packaging). Nevertheless, for a first order approximation one may consider a spatially constant heat conductivity (nearly that of water) when solving the classical heat conduction equation. The heat conduction problem resulting from balance of generated and depleted heat was treated analytically and confirmed experimentally by Andrä *et al* [7, 14]. They considered a spherical region of internal constant heat production—irrespective of whether the heat in that region originates from many homogeneously distributed small particles or is only due to one large object. The transport in the medium outside of that spherical heat production zone may be characterized by the well-known heat conductivity of water. Results of those calculations are summarized in figure 10.

Initially, the temperature inside the heat generation zone grows rapidly with progressing heating time. After that initial rapid rise, temperature increase becomes steadily smaller and a nearly constant temperature is reached within the particle containing zone. Outside of the tumour, the temperature declines rather steep. Reasonably, the results scale with the SHP of the particles.

The heat conduction model shows that the achievable temperature elevation in the tumour depends strongly on the actual size of the heat generation zone. Since the heat production scales with the third power of the radius of the particle containing volume R^3, but the heat depletion with the square R^2, a serious limitation of the heating efficiency occurs with decreasing tumour size. As a result, the maximum temperature achievable with a constant amount of particles will unfortunately be less than the critical value for cell destruction in the particular volume to be heated. A smaller volume—at constant available power—leads to a stronger dissipation of the generated heat into healthy tissue and thus a lower temperature inside the tumour results. Taking this size effect into account, the SHP which is needed to heat up a spherical tumour of radius R loaded with a MNP concentration c to a desired temperature ΔT is given by

$$\mathrm{SHP} = \frac{\Delta T \cdot 3\lambda}{c \cdot R^2}. \tag{13}$$

There, the heat conductivity of tissue λ may be assumed to be 0.64 $\mathrm{WK^{-1}m^{-1}}$, see [97]. Equation (13) supposes that the cell membrane is not a significant barrier to heat flow [177].

The consequences of the critical size effect are illustrated in figure 11, deduced from data of the original paper of Hergt and Dutz [97]. The demand of SHP for obtaining a temperature increase of 15 K (which surely is sufficient for thermoablation) may be read in dependence on tumour size. The power demand is calculated for three different absorber concentrations: For direct intratumoural injection of particles, concentrations of 100 and 10 mg MNP per $\mathrm{cm^3}$ of tumour tissue [155] seem to be practicable. In comparison, for antibody targeting a concentration of not more than 1 mg MNP per $\mathrm{cm^3}$ may be expected [114]. The results show that by intratumoural injection of a typically available MNP having a SHP of a few 100 $\mathrm{W\,g^{-1}}$, the thermoablation treatment of tumours seems to be promising for tumours larger than 5 mm. But for delivering of MNP by antibody targeting a thermoablation effect of MNP for tumours smaller than 15 mm is unrealistic. In comparison, the situation is more favourable for hyperthermia with a temperature increase of only 5 K. Here tumours larger than 3 mm show the necessary temperature increase after direct injection. For antibody targeting the tumour size treatable by hyperthermia cannot be smaller than 10 mm. The curves of figure 11 clearly show that the wish to destroy small metastases by targeted MPH is—at least at the moment—rather unrealistic. In particular, a single tumour cell

filled even completely with MNPs would not experience any temperature increase unless placed under unrealistic high values of SHP. Recent hopes of 'non-thermal' energy transfer on a cellular scale are discussed below.

The predictions of figure 11 were confirmed by investigations of several groups [15, 21, 122, 124, 223]. In the experimental work of Yamada *et al* [223], cancer cell pellets of different sizes (1–40 mm) were heated up to 50 °C for 10 min to obtain complete cell death. It was confirmed that larger tumours require a smaller heat dose to achieve the target temperature. Assuming an available maximum SHP of 1000 W g^{-1} and a MNP concentration of 2 mg cm^{-3}, the treatment of 10 mm tumours seems to be possible. Hedayati *et al* [93] extended the lower pellet size down to clusters of a few thousand cells. They found when using particles showing an SHP of 480 W g^{-1}, that a minimum pellet size of 1.2 mm (250 000 cells and each loaded with 200 pg Fe) was needed to obtain the minimum necessary temperature of 41.3 °C to cause a cytotoxic effect within the cells. In summary, most investigations show that hyperthermia treatment of relatively small tumours in the lower mm-range may only be possible when using MNP with a high SHP above about 500 W g^{-1}.

5.1.1. Present state of SHP. In the last 5–10 years, a notable enhancement of the SHP of MNP was achieved. Ten years ago, SHP of synthetic MNP was typically in the range of 50–200 W g^{-1}. Bacterial magnetosomes with a SHP of around 1000 W g^{-1} [101] set the benchmark for achievable heating power. Nowadays, absolute SHP values of more than 1500 W g^{-1} can be reached. A SHP of 1650 W g^{-1} (measured at $f = 700$ kHz and $H = 24.8$ kA m^{-1}) was reported by Fortin *et al* [71] for particles of 16.5 nm obtained from size dependent fractionation of a sample showing a broader size distribution. However, the reported value was obtained for field parameters clearly out of range of feasible combinations for clinical hyperthermia. While the applied field parameters are crucial for the resulting SHP, a direct comparison of SHP values from different groups measured at varying field parameters is difficult. To allow a better comparison, the measure 'intrinsic loss power' (ILP) was introduced by Pankhurst *et al* [123]. The ILP is defined as the SHP normalized to H^2 and f assuming a corresponding dependence of SHP on these parameters. However, it should be pointed out that this normalization relies on the small amplitude restriction of the Neél relaxation model discussed above. Despite of the fact that this dependence is not appropriate for the whole range of MNP sizes and all applied field strengths and frequencies [26, 137, 157, 226], the ILP may be taken as a rough practical measure for the heating performance of MNP. However to avoid misinterpretations, it is absolutely necessary to consider absolute values of SHP in addition to ILP values, too. For instance, a relatively low SHP measured for small field strength and frequency may result in a high ILP whereas the particles are not suitable for heating since the absolute SHP is too low and the assumed dependency on H and f is not guaranteed. Typical ILP values suitable for heating are in the range from 3 to 4 $nHm^2 kg^{-1}$ and the highest reported value ever is 23.4 $nHm^2 kg^{-1}$ for magnetosomes [101]. Obviously, the natural synthesis by those bacteria is favourable to all technical preparation methods, yet. A recent review on the possible use of magnetosomes for MPH was given by Alphandery *et al* [4].

The state of the art of particle preparation in general is presented in reviews by Barry [17], Kallumadil [123] and Pollert [176] as already discussed in section 3. Newest magnetic iron oxide particle developments reach SHP values of up to 1650 W g^{-1} (ILP = 3.8 $nHm^2 kg^{-1}$) [71], 1500 W g^{-1} (ILP = 4.6 $nHm^2 kg^{-1}$) [137], 1179 W g^{-1} (ILP = 6.1 $nHm^2 kg^{-1}$) [209], 537 W g^{-1} (ILP = 0.4 $nHm^2 kg^{-1}$) [26], and 332 W g^{-1} (ILP = 8.3 $nHm^2 kg^{-1}$) [57]. The last one is the highest ever reported ILP for synthetic particles [176] and was obtained for fractionated multicore nanoparticles [56, 57]. The multicore particles exhibit a magnetic behaviour different from single core particles [137] and have shown promising results for hyperthermia treatment in animal experiments [63].

From a practical point of view of MPH therapy, it is absolutely indispensable that reliable SHP values at defined field parameters are given in data sheets of MNPs. Insofar, measurements of SHP values must be standardized. For most of the SHP values reported in literature, one has to keep in mind that these measurements were carried out on *liquid* samples and, consequently, show a contribution of Brownian relaxation to heating losses. This loss type is not relevant for the real magnetic behaviour of particles administered to tumours because particles bind to tissue immediately after injection [63, 180]. This leads to a reduced thermal dose applied to the tumour.

Many papers deal with refinements of measurement technique for liquid suspensions [10]. However, as demonstrated above in section 2 the measurement of SHP in liquid suspensions is of minor interest for an evaluation of the therapeutic value of particles. Instead, heating power has to be measured in standardized tumour-like dummy tissue, e.g. in gels of appropriate viscosity. Reasonably, standardized values of the field parameters (i.e. amplitude and frequency) should be used. These have to be chosen according to optimum therapy conditions holding the product f.H below the highest physiologically allowable value given below (section 5.4).

5.2. Tissue damage due to temperature elevation

The damaging effect of temperature elevation above the natural physiological level of living cells has been the subject of many investigations and review articles. From this large body of work, a few representative reviews should be mentioned: Falk and Issels (2001) [68], Moroz (2002) [155] and Dewhirst (2003) [51]. Recently, a special issue of the International Journal of Hyperthermia (Volume 29, Number 8, December 2013) was devoted to MPH which should represent the latest state of the art.

Considering the modes of thermal cell damaging two regimes of temperature treatment are occasionally differentiated: The first is hyperthermia where temperatures slightly above the physiological level are applied in human patients. In this temperature range, cytotoxic effects depend on

physiological cell parameters (e.g. acidity or hypoxia). Due to the different metabolism of tumour cells in comparison to healthy cells an increased thermal sensitivity was already expected in the early years of whole body hyperthermia in the sixties of last century. The resulting hope of damaging tumour cells selectively, however, till now was not fulfilled satisfyingly. Therefore, as a second, more radical regime thermoablation is discussed. It refers to the application of elevated temperatures which lead to cell death due to irreparable destruction of molecular constituents of the living cells (mainly cytoplasmic and membrane proteins). Damage at such elevated temperatures is irreversible and cell death may occur after just a few minutes of exposure to heating.

There are different opinions in literature regarding the choice of the temperature elevation under therapy. Hilger *et al* [104] assume that for clinical applications at least 55 °C are necessary. Those authors applied extreme temperature enhancements up to more than 70 °C in animal experiments (e.g. [107]). However, avoiding unnecessary pain under therapy seems to be a serious issue—at least in human therapy. In comparison, results of recently performed clinical trials [118] suggest a temperature enhancement up to about 46 °C to be sufficient.

The death rate of cells in the narrow transition range between physiologically optimum and clearly lethally temperatures depends on nearly all parameters of the cell environment that influence cell metabolism. In particular, there is a coupling to all kinds of cell damaging agents. Consequently, there are many therapeutic attempts to combine any kind of damaging agents, for instance irradiation or chemotherapeutic drugs with temperature elevation [5, 86, 149, 217]. For a combination of irradiation and heat, Dewhirst *et al* [210] found a greater reduction in tumour volume when using a few large thermal doses with higher temperatures than when using a larger number of doses with lower temperatures.

The degree of cell damage is usually proved by determining surviving fractions by means of *in vitro* experiments with cell cultures. In such experiments it was found that in addition to the absolute value of temperature, the duration of the exposure to the elevated temperature plays a crucial role. This has led to suggestions that a 'thermal dose' may be defined, in analogy to what is usually done for irradiation damage. Basic principles of thermal dosimetry and thermal thresholds for tissue damages from hyperthermia were discussed by Dewhirst [51] who reported that above 43 °C the effective exposure time may be halved for each 1 °C temperature elevation. This rule seems to be commonly adapted [215]. Also in one of the most recent clinical studies [118] the concept of the thermal dose is used for application in clinical practice. In a series of first therapeutic trials of hyperthermia, the authors report that a treatment time of 60 min at 43 °C may be halved to 30 min at 44 °C, but the treatment time has to be increased four times to 240 min at 42 °C. For description of the two regimes the authors suggest two exponential laws which are represented in figure 12 for showing the 'isoeffect time' in dependence on the treatment temperature.

Experimental data for thermal damage of different cell types lead to attempts to apply the concepts of thermal activation to hyperthermia [49]. Typical 'activation energies' of 500–600 kJ mole^{-1} were derived from Arrhenius plots. In a recent letter [50] Dewey points out that above the break at 43 °C the 'activation energy' is roughly doubled. However, one should be aware of the suppositions of the Arrhenius equation in reaction rate theory [89, 200]. There, a predominant molecular reaction may be characterized by a typical potential barrier, the so-called activation energy. In contrast, in the case of thermal cell damage several types of bio-reactions are involved and there is a superposition of different reaction paths. The complex picture due the superposition of effects of different physiological parameters is shown in a survey on the cellular and molecular basis of hyperthermia given by Hildebrandt *et al* [103]. Accordingly, the data of figure 12 should be regarded rather as a rule of thumb being valuable for practical therapy planning. Of course, the real temperature of the tumour during the therapy process has to be carefully monitored by thermoprobes and has to be controlled by field amplitude adjustment.

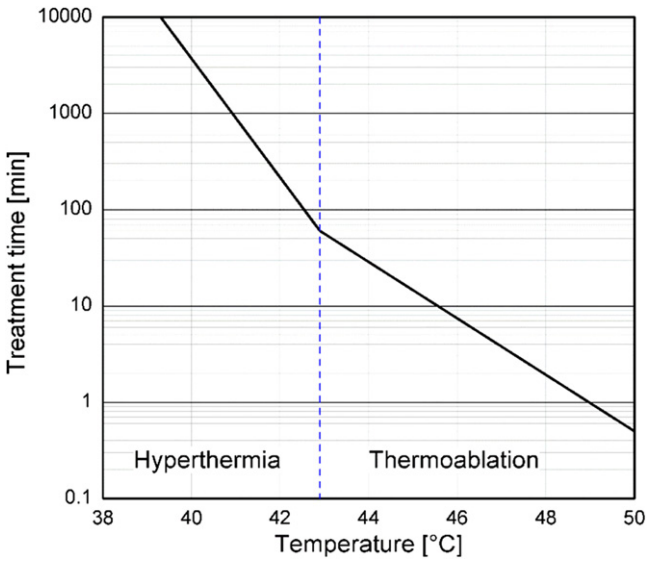

Figure 12. 'Isoeffect time' in dependence on treatment temperature for hyperthermia and thermoablation, according to results of Johannson *et al* [117].

5.3. 'Non-thermal' effects in MPH?

The simulation of the heating efficiency of MNPs by means of a heat conduction model has shown that the temperature rise in small volumes is seriously limited. Considering this obvious drawback of MPH for small heated volumes, the possibility of more effective mechanisms of energy deposition was discussed in literature. Already in the early years of magnetic hyperthermia some authors proclaimed 'intracellular hyperthermia' to be a special highly effective mechanism of tumour destruction. Due to such speculations some unrealistic expectations with respect to the new tumour therapy were induced, in particular by rather popular announcements. The important issue of the possibility of a particularly effective way of tumour cell destruction by particle incorporation was addressed critically by Rabin [177]. He considered very

comprehensively the possibility of nanoscale heat transfer. In summary, his analysis showed no alternative to the classical heat conduction. Rabin has pointed out that cell membranes represent no essential resistance to heat conduction. In particular, he showed that the high effectivity of so-called 'intracellular' hyperthermia occasionally claimed (e.g. [82, 121]) is without any biophysical reason. In principle, Rabin confirmed that the results of Andrä *et al* [7] i.e. common heat conduction mechanism, are valid on the micro-scale of nanoparticle heating, too. Results of classical theory were mainly confirmed by Keblinski *et al* [124].

Nevertheless, recently, some groups claim finding of remarkable temperature elevations on the nanoscale which seem to exceed predictions of classical heat conduction. Interest on excessive temperature enhancement of nanoparticles came from a completely different area of technical nanoparticle applications, e.g. of nanodots or of high-density thermomagnetic recording. Accordingly, already Chen [40] has treated non-local and non-equilibrium heat conduction in the vicinity of nanoparticles. Deviations from macroscopic heat conduction theory have to be expected if the particle radius is small in comparison to the heat-carrier mean free path. For this limiting case, the calculations of Chen indicate a temperature jump at the particle boundary. Indeed, for 3 nm quantum nanodots heated by irradiation Rodrigues *et al* [184] found a threefold rise of the dot temperature in comparison to the predictions of the heat conduction theory. The authors used atomic spectroscopic probes which offer the possibility of nanoscale temperature measurements. The method found interesting applications in cell biology, too. As an example of those local temperature measurements Yang *et al* [225] used quantum dot nano thermometers for demonstrating the effect of Ca^{+}-shocks on the thermogenesis in single living cells under physiological conditions. With respect to hyperthermia, Huang *et al* [108] used the emission of fluorophores bound to the functional particle coating (streptavidin) for thermometry. The authors found an enhancement of the temperature of nanoparticles under the action of an external magnetic ac-field. Nanoparticles were situated on the cell membrane, and simultaneously with the temperature increase a change of the membrane potential was recorded. Remarkably, the temperature increase was observed to be restricted to the fluorescence marker bound to the nanoparticles while markers at the cell Golgi apparatus indicated no cytoplasmic heating. At the same time, the temperature of the bulk cell suspension was proved to be negligible since 'the temperature around the nanoparticle decays too rapidly to cause appreciable bulk heating'. In accordance, Riedinger *et al* [181] report a temperature gradient near the surface of MNPs heated by an alternating magnetic field, which was much steeper than predicted by simulations of thermal conduction. However, the method is rather indirect by using dye-thermolabile groups and high molecular spacers (PEG) coupled to the particle coating. Both, the determination of temperature as well as distance from particle surface need complicate calibration procedures. The more astonishing are the relatively small given error bars of the results of Riedinger *et al.* The temperature outside of the nanoparticles is reported to decline so rapidly that it is already fallen below one tenth in a distance 3 nm apart. This temperature gradient is much steeper than expected for diffusive heat conduction. Probably, the excessive peak temperature of ac-field heated nanoparticles may be caused due to heat-carrier mean free path effects. Strangely, the authors report a linear dependence of the temperature increase on the magnetic field amplitude which may rarely be understood considering the basics of magnetic heating presented above. Methods taking a fluorescence *intensity* as a measure of temperature were criticized by Okabe *et al* [165]. Instead, these authors use fluorescence *lifetime* for imaging of the intracellular temperature distribution and present astonishing observations considering cell metabolism. Unfortunately, no applications of the method to the present problem of intracellular temperature transfer around a heated nanoparticle are known, though the lifetime thermometry appears to be a promising tool.

Considering the importance of defined energy delivery on a sub-cellular scale, further studies are highly desirable to elucidate present lack of understanding. For instance, Hamad-Schifferli *et al* [87] claim a local heating effect on DNA molecules by means of induction heating of extremely small gold nanoparticles. The mechanism is quite unclear as criticized by Keblinski *et al* [124]. With respect to cancer therapy, it should be pointed out that rather than the temperature of the nanoparticle itself, the transition of the temperature elevation to the biological surrounding, e.g. the cell plasma and nucleus is of interest for damaging the tumour. This has to be considered in particular if a step like temperature decrease at the particle surface is observed. On the other hand, measurements of the global temperature of a cell suspension by macroscopic temperature sensors give rarely information on effective energy transfer from nanoparticles to their immediate cellular surrounding. For instance, Zhang *et al* [231] found cell damaging effects using Herceptin guided MNP to malignant human mammary epithelial cells without observing significant temperature increase by means of fibre-optic temperature probes inserted into the wells. Creixell *et al* [43] claim killing of cancer cells by magnetic particle heating 'without a perceptible temperature rise'. However, it seems erroneous to exclude local microscale temperature rise by holding the incubator temperature of the samples constant. In summary, new methods of measuring physical parameters on the sub-cellular length scale proved promising, but energy transfer on this scale has carefully revisited.

Besides the thermal damaging of tumour cells, there exist observations of really non-thermal damaging effects [127]. They show that MNPs oscillating under the influence of an external alternating magnetic field may induce *mechanical damage* in the cell interior. Typically, such cell damage was observed at low frequencies in the order of <100 Hz where thermal effects may surely be excluded.

5.4. Clinical application

Since from the very beginning half a century ago MPH has pursued clearly with the goal of establishing a useful tumour therapy, there are only a few attempts to introduce MPH into

clinical practice till now. Despite of a lot of scientific investigations—to a large extent by means of cell culture experiments—the break-through as a valuable therapy did not succeed until now. Already ten years ago some letters to International Journal of Radiation Oncology Biology (e.g. [51]) addressed the problems with Phase III clinical trials of MPH. In particular, the statement of Dewhirst and Sneed 'New technologies can ill afford to be tested in poorly designed and quality controlled Phase III trials that run the risk of failing to show therapeutic benefit as a result' is valid yet.

5.4.1. Technical implication of MPH Besides the preparation of suitable magnetic particle suspensions, the therapy needs an appropriate magnetic field applicator. For developing the main technical component of an MPH therapy equipment, the ac-field body coil, one started from technical magnetic coil design. Though induction coils are widely used in industry, the technical task was new and challenging since in contrast to those machines a big torso coil has to be driven without any inductive load. This means that nearly the full amount of the considerable electric energy demand has to be depleted by cooling of the coil. A technically satisfying hyperthermia and thermoablation system for clinical application was reported by Gneveckow *et al* [78, 79]. Providing a large region of sufficient field homogeneity the heating may be controlled by proper adjustment of field amplitude and duration of the field exposure. Besides of reliable presettings of therapy parameters a precise online control of the local temperature increase is necessary. By temperature sensors (e.g. optical fibre probes) inserted into the tumour tissue temperature enhancement may be locally measured and eventually adjusted by means of the field amplitude. The latter one has to be chosen carefully being aware of possible side effects due to unwanted inductive heating of healthy tissue.

According to the above presented physical basics of MPH, the heating power is an increasing function of f and H in a wide parameter range. For medical applications, however, enhancement of heating power is restricted by a limitation of the product of f and H for the following reason: The alternating magnetic field for heating up nanoparticles inside the body does not only damage cancerous tissue but also causes an unwanted non-selective heating of healthy tissue due to eddy currents. The absorbed power due to eddy currents is given by

$$P_{ec} = \sigma \cdot G \cdot (H \cdot f \cdot r)^2, \tag{14}$$

where σ is the electrical conductivity of the tissue, G a geometric coefficient and r the radius of the exposed area (∼coil diameter). For limiting a possible overall body heating, a suitable combination of H and f resulting in maximum heating power has to be chosen taking into account the magnetic properties of the nanoparticles to be used. To prevent harmful effects of electromagnetic fields on the human body, when exposing the body to an alternating magnetic field, an upper limit for the product of frequency and amplitude should be considered. In an experimental study [13], it was found that for a coil of 30 cm in diameter, test persons were able to 'withstand the treatment for more than 1 h without major discomfort' if the product of frequency and field strength did not exceed $4.85 \cdot 10^8\ \mathrm{Am^{-1}\,s^{-1}}$. Taking into account the relationship between exposed area and absorbed power, the given limit might be exceeded by a factor of 10 for hyperthermia treatment of a serious illness with a smaller coil (typically around 10 cm). It was confirmed by the first clinical trials [118] that field amplitudes up to $10\ \mathrm{kA\,m^{-1}}$ at a frequency of 100 kHz will be tolerated. Under these restrictions, tailor-made particles which show maximum magnetic losses for feasible combinations of frequency and amplitude are necessary.

In addition to eddy current effects, spontaneous nerve stimulations also may occur in living tissue [28]. These stimulations are due to induced potentials at neural cells and can lead to uncontrolled movement of limbs and phantom pain, especially when the frequency is below 100 kHz [29]. In the last 15 years, a lot of time was spent investigating such effects. Stimulation thresholds for different types of tissue were determined (e.g., [91, 179]) as summarized by Pankhurst *et al* [172]. As a result from these findings, it is recommended that the smallest possible coil dimensions be used to generate the alternating field and/or focussed fields be applied to minimize the eddy currents in healthy or in tumour tissue.

Besides of the overall inductive body heating to be minimized, the selectivity of MPH is only satisfying if the particle distribution matches the tumour tissue suitably. MPH is aimed at replacing surgery but the selectivity of this method depends on the success of placing the heat sources suitably in tumour tissue. As shown by the results of figure 10, the excess temperature falls to normal body temperature rather rapidly within a few millimetres outside of the nanoparticle bearing zone. The most serious practical problem of MPH tumour therapy is to achieve the matching of the nanoparticle distribution with the tumour shape. Even if the materials optimization and the technical problems are solved satisfyingly, the main problem remains, how to appropriately administer the nanoparticle suspension to the tumour. The administration of the particles to the body is a very sensitive point of hyperthermia. On the one hand, there are several medical risks due to toxic effects or embolization, and on the other hand, after a possible agglomeration of particles during administration the heating power of nanoparticles may decrease, due to magnetic interactions between them.

5.4.2. Particle administration. The most direct method of particle administration is the injection into the tumour tissue. Though injection methods are widely used in medicine the present task is new insofar as different from all classical applications a highly localized tissue depot of the injected fluid is wanted. Since the temperature elevation caused by the external alternating magnetic field is mainly confined to tissue regions containing magnetic particles in sufficient concentration, the tissue distribution of the applied particle suspension should fit the tumour shape. At a first glance one

may assume, that where particle concentration is above the detection limit by diagnostic methods (e.g. x-ray tomography) a therapeutic effect may be expected. However, there are serious practical difficulties for achieving an adequate particle distribution. Of course, the nanoparticle suspension is not homogeneously soluble in organic tissue. During injection it rather displaces the organic matter while distributing itself along of weakest links of the structurally inhomogeneous tissue. Already in first simple injection experiments into pork muscle pieces [106] difficulties with the suspension spread in tissue became obvious. Much more pronounced were these difficulties with model tumours in mice. Since tumour tissue is tighter than healthy one, the suspension tends to escape the tumour and spread out into the normal tissue which is softer and differently textured than the relatively tight tumour tissue. Accordingly, very inhomogeneous, unpredictable quasi fractal distribution patterns of the suspensions are observed. Due to these problems it is even for a globular, well bound tumour difficult to achieve a homogeneous injection. The problems increase if the tumour grows inhomogeneously infiltrating healthy tissue. It is well known, that the tumour shape may remarkably deviate from spherical shape. The cancer may send extended protuberances into the healthy tissue.

Matching an infiltrative growing tumour (for instance, often occurring for glioblastoma) by injection of a MNP suspension seems to be impossible. In particular, if the injection is performed too fast, a large part of the suspension leaks uncontrollable out of the tumour region. Therefore, in recent clinical trials [117] the suspension is infiltrated slowly at different sites of the tumour (multipoint infiltration). Considering the risk of unfavourable particle distribution, it is indispensable, to check the particle distribution after injection by suitable diagnostic means. Knowing the spatial distribution of magnetic particles one may calculate the temperature increase using the SHP according to the above discussed physical principles. Accordingly, in the clinical trials of Johannsen *et al* the injection pattern was planned before treatment of prostate cancer on the base of 3D-imaging of the tumour. An optimization algorithm to determine the optimum heating patterns induced by multiple nanoparticle injections in tumour models with irregular geometries was presented by Salloum *et al* [188]. Nevertheless, under the therapy, the real 3D temperature distribution in the tumour has to be controlled carefully. The adequate filling of a tumour with nanoparticles remains one of the most serious problems of the MPH therapy. Since the particle distribution cannot fit a complicate tumour shape properly, the elimination has to consider keeping a security fringe in healthy tissue. In this case the situation is similar to tumour elimination by surgery.

Of course, direct injection is applicable only for single tumours being detectable by modern cancer diagnostics. The detection limit depends on tumour type and location, but will be not better than about 3 mm (e.g. in the case of breast carcinoma detected by means of mammography). For this size, according to the data of figure 11, no problems should arise to find nanoparticle types of adequate heating power which kill tumour cells reliably. But, one has to keep in mind that the temperature pattern under magnetic field excitation reflects the actual concentration distribution of nanoparticles. Inhomogeneities may cause hot spots on the one hand or unheated regions with surviving tumour cells on the other. Preplanning of the multipoint injection pattern has to take into account besides normal heat conduction also the blood circulation near the tumour. Continuous heat conduction may be disturbed by blood vessels which may result in an increase of the depletion of heat from the heated tumour region—and consequently may cause a decrease of the attainable peak temperature. The blood perfusion of the tumour may be modelled by means of the so-called bio-heat equation [15, 75, 80, 113, 163, 199]. Results show a strong dependency of tumour temperature on the special vessel configuration, in particular if larger blood vessels are involved. In particular in this case, besides a precise planning of the magnetic field amplitude and treatment duration an *in situ* control of the temperature distribution by an array of probes is necessary (e.g. [119]). The latter authors report as limiting factors of their approach '*patient discomfort at high magnetic field strengths and irregular intratumoural heat distribution*'. They estimate that since '*there is no technique available either for direct real-time visual control of the magnetic fluid injection or for reliable imaging of cancer within the prostate … selective ablation of cancer cells while spearing healthy tissue is not yet possible*'. In general, the latter one appears to be the most important obstacle for transition of MPH into clinical practice. Considerable efforts for controlling the therapy are essentially since the practical difficulties of realizing a suitable particle distribution are obviously enormous. Since MPH is presently restricted to larger tumours an additional problem arises which in the case of surgery does not exist. As a result of MPH a considerable amount of necrotic material remains, the elimination of which has to be achieved by the patients organism itself.

Considering the practical difficulties with the direct injection method and the related restrictions with respect to the tumour size one may not wonder that transition of MPH into clinical practice proceeds so sluggish. In particular, considering the limitation of the direct injection method to single tumours in a progressing state, other modalities of particle administration were searched.

5.4.3. Targeting. As alternatives to the administration of MNPs by direct injection, ideas emerged to let find nanoparticles itself their way to the tumour by natural physiological means. One could imagine an enhanced uptake of particles in cancerous tissue due to the tumour angiogenesis. The enrichment effect may be expected in analogy to the enrichment of Gd-contrast agents, which may lead to an initial contrast enhancement providing an improved sensitivity for the detection of breast tumours [70]. In analogy, MNPs shall be delivered to the tumour by transport in supplying blood vessels into which the nanoparticle suspension has to be injected. In the case of intra-arterial injection the danger of embolization exists

which, however, also was suggested to be used intentionally for tumour damaging ('arterial embolization hyperthermia', see, e.g. [155]). Besides, with the transport of nanoparticles in blood vessels other problems arise, for instance elimination by phagocytosis or extravasation into interstitial compartment.

The behaviour of MNPs in the blood circulation system was intensively investigated with respect to their use as contrast agents in the field of magnetic resonance imaging (MRI). Since in comparison to conventional paramagnetic Gd-based contrast agents superparamagnetic particles produce much larger local magnetic fields, a corresponding contrast change may be expected [32]. The most important parameter for the destiny of nanoparticles after supply into the vascular system is the mean particle size. Smallest objects below about 10 nm diameter may leak out of blood vessels and distribute in extracellular fluid (therefore termed occasionally ECF agents). In a diameter range of 10–50 nm a prolonged intravascular circulation time arises which ensures great utility of so-called blood-pool agents in MR angiography. In particular, site specific MRI contrast agents should have a long circulation time prerequisite of sufficient accumulation on a specific target site. For larger particle size in the range of 50–150 nm, particle elimination by phagocytizing cells is most effective. Therefore this group of contrast agents addresses diagnostics of organs of the reticulo-endothelial system (e.g. liver, spleen, bone marrow, lymphatic system). A special group are contrast agents for diagnostics of the gastrointestinal tract using mainly relative large particles of 0.3–3 μm which must be protected by suitable coatings against rapid excretion. For an overview on biomedical application of contrast agents see for instance La Conte *et al* [132]. Data of commercially available superparamagnetic iron oxide based contrast media are compiled in a review paper of Taupitz *et al* [205]. A general drawback of all those delivery processes commonly called 'passive targeting' is the too rapid clearing from the blood circulation system.

Diagnostics by means of MNPs is not yet restricted to NMR tomography. MPI is an emerging novel imaging modality which enables visualization of MNP loaded biological structures [27, 33, 76]. One promising goal in MPH seems to be the combination of diagnostics and therapy by using the same MNPs for contrast enhancement and hyperthermia as well. The idea of using MNPs besides for diagnostics for therapy, too, already has lead to the new acronym 'theranostics'. However, MNP properties for MRI diagnostics and for hyperthermia are all too different. Most effective particle diameters for hyperthermia (cf figure 6) lead to large signal distortion in MRI due to their large magnetic moment.

In relation to the effectiveness of MPH and the appropriate particle size to be used in the case of direct injection, also a possible 'wash-out' of particles out of the tumour was argued. However, as long as particle diameter is not in the range of ECF agents this objection is not relevant. In contrast, some kind of tattooing the tumour by the black suspension has to be expected. Indeed, in trials of MPH treatment of prostate carcinoma [119] it was found that particles are retained in the treated tissue well beyond the treatment interval and are detectable by x-ray tomography even after one year.

The useful particle diameter of so-called blood pool agents discussed above comprises besides the magnetic iron oxide core an organic coating (e.g. dextran), too. This is, on the one hand, necessary for stabilizing the aqueous particle suspensions against particle aggregation. On the other hand, the coating is the boundary to the physiological environment and accordingly it is important for possible interactions with proteins (e.g. immunoglobulins of the blood plasma). For instance, hydrophilic coatings like dextran help to prevent particle elimination by macrophages. Moreover, the coating may be functionalized by bioactive molecular groups e.g. tumour specific antibodies for receptor specific targeting. While experimental investigations are carried out commonly on well defined diluted aqueous suspensions *in vitro*, modifications may be expected for particles in dense tissue for instance when clustering and sticking on cell membranes in a tumour. At high local particle concentrations applied in MPH, interactions discussed above (section 4.3) have to be taken into consideration.

For improving the site specificity of MPH the labelling of magnetic particles with target-specific ligands (e. g. antibodies) seems to be promising, e. g. patent application of Handy *et al* [88]. The visionary idea behind this antibody targeting is the automatic loading of tumours smaller than the diagnostic limit of 3 mm with magnetic particles. This loading shall be obtained by specific binding of systemically applied antibody-labelled MNP to the corresponding tumour tissue [46, 47]. One hopes to eliminate undetected metastases with the help of hyperthermia and even coupling of MNPs to vagabonding tumour cells. Although active targeting is often mentioned in literature, till now only preliminary results of this appealing approach are known. The targeting efficiency, i.e. the concentration enhancement on the tumour site with respect to the magnetic particle concentration of inner organs, was not satisfyingly investigated for remote (e.g. intra-arterial) particle application. However, the concentrations are expected to be rather low. Accordingly, for achieving a useful heating effect one would need a considerable enhancement of the SHP of MNPs. Following the discussion given above in relation to figure 11, the demand of SHP for heating targets in this size range would be enormous. The treatment of cell clusters (100 μm) or even single cells (15 μm) is illusionary, at present. In particular, a single tumour cell filled even completely with MNPs would experience any temperature increase only under unrealistic high values of SHP. From these findings, one has to conclude that so-called 'intracellular hyperthermia' [82, 121] seems to be unachievable due to the unrealistically large amount of heating power necessary to obtain a suitable temperature increase.

Besides the described passive and active modalities of tumour targeting by MNPs, experiments were performed using external magnets in order to assist nanoparticles in finding their way to the tumour. Generally, the method has limited targeting efficiency. It is hampered by the fact that with extra-corporal magnets the centre of attraction for the

particles cannot be positioned within the body. According to a basic property of magnetic fields a local maximum of field strength cannot occur in a source-free space region. This means, that with extra-corporal magnets the force lines are directed to the body surface. This is really useful only in the case of skin cancer for which however other therapy methods than MPH are favourable. Otherwise, for concentrating MNP on a site inside the body properly positioned magnets have to be implanted. As a further drawback, one has to expect insufficient targeting for superparamagnetic particles due to their very low magnetic moment. On the other hand, for larger single domain particles there is the tendency of agglomeration with the hazard of unintended embolization.

In summary, passive as well as active targeting of tumour cells in the human body at present appears to be as visionary as illusionary. Accordingly, therapy-aimed research activities are rare. A vast of investigations is performed by *in vitro* experiments with cell cultures. Another big part of research is devoted to *in vivo* experiments using intra-tumoural injection in animals (e.g. [107, 183]). Unfortunately, many animal experiments are of rather low benefit for useful application of MPH in human medicine. Clinical trials are yet rare and restricted to MNP administration by direct injection.

A special strategy of tumour damage is the coupling of hyperthermia with chemical or irradiational damaging of tumour cells. It seems to be a very useful strategy since nonlinear superposition mechanisms may arise. The complementary agent—be it chemical or radioactive—has to be coupled to the coating of the MNPs. There exists a multitude of opportunities of functionalization of MNPs with differently active compounds. Since the vast number of investigations in literature exceeds the focus of the present review, only the coupling of cisplatin [175] should be called as an example. Without doubt the functionalization of the magnetic particle coating offers many chances for enhancing the efficiency of MPH.

Considering the discussed difficulties to hit the complete tumour volume by means of direct particle injection on the one hand and the very low targeting efficiency of systemic particle administration on the other hand, one may anticipate a combination of both as a useful treatment. MNPs being functionalized with tumour specific antibodies as well as with tumour damaging agents (e.g. cisplatin) have to be injected into the tumour by means of slow multipoint infiltration. In this case the transport paths of the tumour marker bearing nanoparticles to their targets are very short in comparison to systemic administration. Accordingly a rather high concentration at the target site may be expected. After appropriate waiting time the particle distribution may be controlled and the field treatment may be started. In this way, also infiltrative growing tumours as well as neighboured metastases may be adequately filled by MNPs. As further improvements of therapy practice, modifications of the particle injection technique are imaginable.

6. Conclusions

Already Gilchrist [74] was very optimistically considering the therapeutic application of his new method in man. Despite of repeated, optimistic reports in public media, almost half a century passed till first clinical trials with human patients were initiated. Though many questions are open and various restrictions became obvious, one may state without doubt that research on MPH in the past decade has led to a much more profound understanding of the whole topic. Significant progress has occurred in most of the important aspects of this new cancer therapy. The complexity of hyperthermia is obvious and it demands a careful and comprehensive interpretation of the results and their correlations in order to find strategies for further improvement of the present state of the art in hyperthermia. As a typically interdisciplinary object, MPH involved nearly all types of nature scientists from physicists, chemists and biologists to engineers of material science and electrotechnique—with the obviously unavoidable misunderstandings and controversies between them. Now, after long time of scientific development, physicians in clinics are due to apply the new therapy to the benefits of cancer patients.

Regarding the special antitumour agent of MPH—the heat generated by magnetic means—a basic physical understanding has been accomplished between different professions—not without occasional worries. The path towards an increase of the SHP has become clear while its principal limitations became obvious. Magnetic particle heating for tumour thermotherapy is based on hysteresis loss mechanisms that occur when MNPs are exposed to an external alternating field. The magnetic properties of particles are affected by a lot of factors, in particular susceptibility and coercivity. Main control elements are particle size and size distribution. If optimally adapting the particle diameter to the applied field amplitude and frequency, the highest hysteresis losses are obtained for monodisperse particles.

For the preparation of MNPs with tailored properties an arsenal of various physical, chemical and biological methods was elaborated. Though some people believe ‘there is much room for improving the heating efficiency of MNP´s’ [83] no wonders may be expected, yet. Chances for improvement of the SHP may exist by using the natural synthesis of perfect magnetite nanocrystals by bacteria. Also the increase of the magnetic moment would improve SHP. However, FeCo alloys which show the highest known saturation magnetization need careful protection against the oxidizing power of aqueous suspensions. Considering the technical implementation of the therapy, only few place for sophisticated improvements remains, too. Here, a more focused magnetic field application under reduction of the eddy current load of the patient would be desirable.

As a serious restriction of the efficiency of present MPH proved the problem to achieve a temperature elevation not only in the nanoparticle itself but far away (on a nanometre scale!) in order to disturb the metabolism of a tumour cell. Taking into account an increasing surface-to-volume ratio for decreasing tumour size, particles with a very high

heating power would be necessary for the treatment of small tumours, metastases or even vagabonding tumour cells. The key problem of the new therapy is the realization of an adequate particle supply to the tumour tissue, a problem which became clear already decades ago. Here, chances of active targeting by means of tumour markers raised hope. However, despite of many scientific activities with *in vitro* experiments using cell cultures it is quite unclear how to enhance the targeting efficiency in the patient's body.

It is unlikely that with MPH an all purpose cancer therapy will be found, instead each situation needs its own solution. In principle MPH has the potential to find its way into standard medical procedures as may be hoped from the first clinical trials with treatment of prostate cancer [119]. However, considering the treatment of the very problematic glioblastoma [147, 149] it seems to be at present a questionable optimistic opinion 'to expect great breakthroughs in medical science' [83].

In summary, the answer to the question put in the title 'MPH—a promising tumour therapy?' presently is: 'Not yet!' Physicists, in particular magneticians, have elucidated the scientific basis of MPH. Chemists have elaborated different ways towards production of better nanoparticles. Technicians have provided generators and coil arrangements ready for patient´s treatment. Now, biologists and above all medics are in the duty to settle the remaining problems on the way to a useful cancer therapy. There, the main topic remains to be solved, yet: Adequate particle administration to the tumour in the human body.

Acknowledgements

The authors thank Professor Wilfried Andrä (Jena) for fruitful discussions and critical reading of the manuscript. Their special thanks go to Alexander E Brown (Jena) for proofreading the article.

References

[1] Adams J D and Soh H T 2009 Perspectives on utilizing unique features of microfluidics technology for particle and cell sorting *J. Lab. Autom.* **14** 331–40
[2] Aharoni A 1996 *Introduction to the Theory of Ferromagnetism* (Oxford: Clarendon Press)
[3] Alexiou C, Arnold W, Klein R J, Parak F G, Hulin P, Bergemann C, Erhardt W, Wagenpfeil S and Lubbe A S 2000 Locoregional cancer treatment with magnetic drug targeting *Cancer Res.* **60** 6641–8 http://cancerres.aacrjournals.org/content/60/23/6641.full
[4] Alphandery E, Chebbi I, Guyot F and Durand-Dubief M 2013 Use of bacterial magnetosomes in the magnetic hyperthermia treatment of tumours: a review *Int. J. Hyperthermia* **29** 801–9
[5] Alvarez-Berrios M P, Castillo A, Mendez J, Soto O, Rinaldi C and Torres-Lugo M 2013 Hyperthermic potentiation of cisplatin by magnetic nanoparticle heaters is correlated with an increase in cell membrane fluidity *Int. J. Nanomed.* **8** 1003–13
[6] Anderson P W 1950 Antiferromagnetismm—theory of superexchange interaction *Phys. Rev.* **79** 350–6
[7] Andra W, d'Ambly C G, Hergt R, Hilger I and Kaiser W A 1999 Temperature distribution as function of time around a small spherical heat source of local magnetic hyperthermia *J. Magn. Magn. Mater.* **194** 197–203
[8] Andrae W, Haefeli U O, Hergt R and Misri R 2007 *Handbook of Magnetism and Advanced Magnetic Materials* ed H Kronmueller and S S P Parkin (Chichester: Wiley) pp 2536–68
[9] Andres Verges M, Costo R, Roca A G, Marco J F, Goya G F, Serna C J and Morales M P 2008 Uniform and water stable magnetite nanoparticles with diameters around the monodomain-multidomain limit *J. Phys. D: Appl. Phys.* **41** 134003
[10] Andreu I and Natividad E 2013 Accuracy of available methods for quantifying the heat power generation of nanoparticles for magnetic hyperthermia *Int. J. Hyperthermia* **29** 739–51
[11] Ardenne M V 1994 Principles and concept 1993 of the systemic cancer multistep therapy (SCMT) *Strahlenther. Onkol.* **170** 581–9
[12] Arruebo M, Valladares M and Gonzalez-Fernandez A 2009 Antibody-conjugated nanoparticles for biomedical applications *J. Nanomater.* 439389
[13] Atkinson W J, Brezovich I A and Chakraborty D P 1984 Usable frequencies in hyperthermia with thermal seeds *IEEE Trans. Biomed. Eng.* **31** 70–5
[14] Attaluri A, Ma R, Qiu Y, Li W and Zhu L 2011 Nanoparticle distribution and temperature elevations in prostatic tumours in mice during magnetic nanoparticle hyperthermia *Int. J. Hyperthermia* **27** 491–502
[15] Bagaria H G and Johnson D T 2005 Transient solution to the bioheat equation and optimization for magnetic fluid hyperthermia treatment *Int. J. Hyperthermia* **21** 57–75
[16] Bakoglidis K D, Simeonidis K, Sakellari D, Stefanou G and Angelakeris M 2012 Size-dependent mechanisms in AC magnetic hyperthermia response of iron-oxide nanoparticles *IEEE Trans. Magn.* **48** 1320–3
[17] Barry S E 2008 Challenges in the development of magnetic particles for therapeutic applications *Int. J. Hyperthermia* **24** 451–66
[18] Baumgartner J, Carillo M A, Eckes K M, Werner P and Faivre D 2014 Biomimetic magnetite formation: from biocombinatorial approaches to mineralization effects *Langmuir* **30** 2129–36
[19] Bazylinski D A and Frankel R B 2004 Magnetosome formation in prokaryotes *Nat. Rev. Microbiol.* **2** 217–30
[20] Bazylinski D A, Garrattreed A J and Frankel R B 1994 Electron-microscopic studies of magnetosomes in magnetotactic bacteria *Microsc. Res. Tech.* **27** 389–401
[21] Bellizzi G and Bucci O M 2010 On the optimal choice of the exposure conditions and the nanoparticle features in magnetic nanoparticle hyperthermia *Int. J. Hyperthermia* **26** 389–403
[22] Berkov D V 1996 Numerical simulations of quasistatic remagnetization processes in fine magnetic particle systems *J. Magn. Magn. Mater.* **161** 337–56
[23] Berret J F, Sandre O and Mauger A 2007 Size distribution of superparamagnetic particles determined by magnetic sedimentation *Langmuir* **23** 2993–9
[24] Bertotti G 1998 *Hysteresis in Magnetism* (New York: Academic)
[25] Bhagat A A S, Kuntaegowdanahalli S S and Papautsky I 2008 Continuous particle separation in spiral microchannels using dean flows and differential migration *Lab Chip* **8** 1906–14
[26] Bordelon D E, Cornejo C, Gruttner C, Westphal F, DeWeese T L and Ivkov R 2011 Magnetic nanoparticle heating efficiency reveals magneto-structural differences when characterized with wide ranging and high amplitude alternating magnetic fields *J. Appl. Phys.* **109** 1249041–8

[27] Borgert J *et al* 2013 Perspectives on clinical magnetic particle imaging *Biomed. Tech.* **58** 551–6
[28] Borrelli N F, Luderer A A and Panzarino J N 1984 Hysteresis heating for the treatment of tumors *Phys. Med. Biol.* **29** 487–94
[29] Brezovich I A 1988 Low frequency hyperthermia *Med. Phys. Monogr.* **16** 82–111
[30] Brezovich I A and Young J H 1981 Hyperthermia with implanted electrodes *Med. Phys.* **8** 79–84
[31] Brown W F 1963 Thermal fluctuations of a single-domain particle *Phys. Rev.* **130** 1677–86
[32] Bulte J W, DeCuyper M, Despres D, Brooks R A, Jordan E K and Frank J A 1997 Short-versus long-circulating magnetoliposomes as bone marrow-seeking MR imaging contrast agents *Radiology* **205** 1298
[33] Busch C J 1866 Einfluss heftiger Erysipeln auf organisierte Neubildungen *Verhandlungen Des Naturhistorischen Vereins Der Preussischen Rheinlande und Westphalens* ed C J Andrä (Bonn: Max Cohen und Sohn) pp 28–33
[34] Carpino F, Zborowski M and Williams P S 2007 Quadrupole magnetic field-flow fractionation: a novel technique for the characterization of magnetic nanoparticles *J. Magn. Magn. Mater.* **311** 383–7
[35] Castro L L, da Silva M F, Bakuzis A F and Miotto R 2005 Aggregate formation on polydisperse ferrofluids: a Monte Carlo analysis *J. Magn. Magn. Mater.* **293** 553–8
[36] Cetas T C, Hevezi J M, Manning M R and Ozimek E J 1982 *Cancer Therapy by Hyperthemia, Drugs, and Radiation* (Bethesda, MD: National Cancer Institute) pp 505–7
[37] Chanteau B, Fresnais J and Berret J F 2009 Electrosteric enhanced stability of functional sub-10 nm cerium and iron oxide particles in cell culture medium *Langmuir* **25** 9064–70
[38] Chantrell R W, Bradbury A, Popplewell J and Charles S W 1980 Particle cluster configuration in magnetic fluids *J. Phys. D: Appl. Phys.* **13** L119–22
[39] Chatterjee J, Haik Y and Chen C J 2003 Size dependent magnetic properties of iron oxide nanoparticles *J. Magn. Magn. Mater.* **257** 113–8
[40] Chen G 1996 Nonlocal and nonequilibrium heat conduction in the vicinity of nanoparticles *J. Heat Transfer* **118** 539–45
[41] Coffey W T and Kalmykov Y P 2012 Thermal fluctuations of magnetic nanoparticles: fifty years after Brown *J. Appl. Phys.* **112**
[42] Coyle S T and Scheinfein M R 1998 Magnetic ordering in Co films on stepped Cu(100) surfaces *J. Appl. Phys.* **83** 7040–2
[43] Creixell M, Bohorquez A C, Torres-Lugo M and Rinaldi C 2011 EGFR-targeted magnetic nanoparticle heaters kill cancer cells without a perceptible temperature rise *ACS Nano* **5** 7124–9
[44] de la Presa P, Luengo Y, Multigner M, Costo R, Morales M P, Rivero G and Hernando A 2012 Study of heating efficiency as a function of concentration, size, and applied field in gamma-Fe2O3 nanoparticles *J. Phys. Chem. C* **116** 25602–10
[45] Debye P 1929 *Polar Molecules* (New York: Dover)
[46] DeNardo S J, DeNardo G L, Miers L A, Natarajan A, Foreman A R, Gruettner C, Adamson G N and Ivkov R 2005 Development of tumor targeting bioprobes (In-111-chimeric L6 monoclonal antibody nanoparticles) for alternating magnetic field cancer therapy *Clin. Cancer Res.* **11** 7087S
[47] DeNardo S J, DeNardo G L, Natarajan A, Miers L A, Foreman A R, Gruettner C, Adamson G N and Ivkov R 2007 Thermal dosimetry predictive of efficacy of In-111-ChL6 nanoparticle AMF-induced thermoablative therapy for human breast cancer in mice *J. Nucl. Med.* **48** 437–44 http://jnm.snmjournals.org/content/48/3/437.full.pdf+html
[48] Dennis C L, Jackson A J, Borchers J A, Hoopes P J, Strawbridge R, Foreman A R, van Lierop J, Gruttner C and Ivkov R 2009 Nearly complete regression of tumors via collective behavior of magnetic nanoparticles in hyperthermia *Nanotechnology* **20** 395103
[49] Dewey W C 1994 Arrhenius relationships from the molecule and cell to the clinic *Int. J. Hyperthermia* **10** 457–83
[50] Dewey W C 2009 Arrhenius relationships from the molecule and cell to the clinic *Int. J. Hyperthermia* **25** 3–20
[51] Dewhirst M W, Viglianti B L, Lora-Michiels M, Hanson M and Hoopes P J 2003 Basic principles of thermal dosimetry and thermal thresholds for tissue damage from hyperthermia *Int. J. Hyperthermia* **19** 267–94
[52] Doss J D 1975 Use of rf fields to produce hyperthermia in animal tumors *Proc. Int. Symp. Cancer Therapy by Hyperthermia and Radiation* pp 226–7
[53] Douple E B, Strohbehn J W, Bowers E D and Walsh J E 1979 Cancer-therapy with localized hyperthermia using an invasive microwave system *J. Microw. Power Electromagn. Energy* **14** 181–6
[54] Dunin-Borkowski R E, McCartney M R, Posfai M, Frankel R B, Bazylinski D A and Buseck P R 2001 Off-axis electron holography of magnetotactic bacteria: magnetic microstructure of strains MV-1 and MS-1 *Eur. J. Mineral.* **13** 671–84
[55] Dunlop D J 1971 Magnetic properties of fine-particle hematite *Ann. Geophys.* **27** 269
[56] Dutz S, Andrae W, Hergt R, Mueller R, Oestreich C, Schmidt C, Toepfer J, Zeisberger M and Bellemann M E 2007 Influence of dextran coating on the magnetic behaviour of iron oxide nanoparticles *J. Magn. Magn. Mater.* **311** 51–4
[57] Dutz S, Clement J H, Eberbeck D, Gelbrich T, Hergt R, Mueller R, Wotschadlo J and Zeisberger M 2009 Ferrofluids of magnetic multicore nanoparticles for biomedical applications *J. Magn. Magn. Mater.* **321** 1501–4
[58] Dutz S, Hayden M E, Schaap A, Stoeber B and Haefeli U O 2012 A microfluidic spiral for size-dependent fractionation of magnetic microspheres *J. Magn. Magn. Mater.* **324** 3791–8
[59] Dutz S and Hergt R 2012 The role of interactions in systems of single domain ferrimagnetic iron oxide nanoparticles *J. Nano-Electron. Phys.* **4** 20101–7
[60] Dutz S and Hergt R 2013 Magnetic nanoparticle heating and heat transfer on a microscale: basic principles, realities and physical limitations of hyperthermia for tumour therapy *Int. J. Hyperthermia* **29** 790–800
[61] Dutz S, Hergt R, Muerbe J, Mueller R, Zeisberger M, Andrae W, Toepfer J and Bellemann M E 2007 Hysteresis losses of magnetic nanoparticle powders in the single domain size range *J. Magn. Magn. Mater.* **308** 305–12
[62] Dutz S, Hergt R, Murbe J, Topfer J, Muller R, Zeisberger M, Andra W and Bellemann M E 2006 Magnetic nanoparticles for biomedical heating applications *Z. Phys. Chem.* **220** 145–51
[63] Dutz S, Kettering M, Hilger I, Muller R and Zeisberger M 2011 Magnetic multicore nanoparticles for hyperthermia-influence of particle immobilization in tumour tissue on magnetic properties *Nanotechnology* **22** 265102
[64] Dutz S, Kuntsche J, Eberbeck D, Muller R and Zeisberger M 2012 Asymmetric flow field-flow fractionation of superferrimagnetic iron oxide multicore nanoparticles *Nanotechnology* **23** 355701
[65] Eberbeck D, Dennis C L, Huls N F, Krycka K L, Gruttner C and Westphal F 2013 Multicore magnetic nanoparticles for magnetic particle imaging *IEEE Trans. Magn.* **49** 269–74
[66] Eberbeck D and Trahms L 2011 Experimental investigation of dipolar interaction in suspensions of magnetic nanoparticles *J. Magn. Magn. Mater.* **323** 1228–32
[67] Eggeman A S, Majetich S A, Farrell D and Pankhurst Q A 2007 Size and concentration effects on high frequency hysteresis of iron oxide nanoparticles *IEEE Trans. Magn.* **43** 2451–3

[68] Falk M H and Issels R D 2001 Hyperthermia in oncology *Int. J. Hyperthermia* **17** 1–18
[69] Ferrari R *et al* 2014 Integrated multiplatform method for *in vitro* quantitative assessment of cellular uptake for fluorescent polymer nanoparticles *Nanotechnology* **25** 045102
[70] Folkman J 1985 Tumor angiogenesis *Adv. Cancer Res.* **43** 175–203
[71] Fortin J-P, Wilhelm C, Servais J, Menager C, Bacri J-C and Gazeau F 2007 Size-sorted anionic iron oxide nanomagnets as colloidal mediators for magnetic hyperthermia *J. Am. Chem. Soc.* **129** 2628–35
[72] Garanin D A and Kachkachi H 2003 Surface contribution to the anisotropy of magnetic nanoparticles *Phys. Rev. Lett.* **90** 655041–4
[73] Gerber R 1984 Magnetic filtration of ultra-fine particles *IEEE Trans. Magn.* **20** 1159–64
[74] Gilchrist R K, Medal R, Shorey W D, Hanselman R C, Parrott J C and Taylor C B 1957 Selective inductive heating of lymph nodes *Ann. Surg.* **146** 596–606
[75] Giordano M A, Gutierrez G and Rinaldi C 2010 Fundamental solutions to the bioheat equation and their application to magnetic fluid hyperthermia *Int. J. Hyperthermia* **26** 475–84
[76] Gleich B and Weizenecker R 2005 Tomographic imaging using the nonlinear response of magnetic particles *Nature* **435** 1214–7
[77] Gloeckl G, Hergt R, Zeisberger M, Dutz S, Nagel S and Weitschies W 2006 The effect of field parameters, nanoparticle properties and immobilization on the specific heating power in magnetic particle hyperthermia *J. Phys.: Condens. Matter* **18** S2935–49
[78] Gneveckow U, Jordan A, Scholz R, Bruss V, Waldofner N, Ricke J, Feussner A, Hildebrandt B, Rau B and Wust P 2004 Description and characterization of the novel hyperthermia- and thermoablation-system MFH (R) 300F for clinical magnetic fluid hyperthermia *Med. Phys.* **31** 1444–51
[79] Gneveckow U, Jordan A, Scholz R, Eckelt L, Maier-Hauff K, Johannsen M and Wust P 2005 Magnetic force nanotherapy *Biomed. Tech. (Berlin)* **50** 92–3
[80] Golneshan A A and Lahonian M 2011 The effect of magnetic nanoparticle dispersion on temperature distribution in a spherical tissue in magnetic fluid hyperthermia using the lattice boltzmann method *Int. J. Hyperthermia* **27** 266–74
[81] Gonzales-Weimuller M, Zeisberger M and Krishnan K M 2009 Size-dependant heating rates of iron oxide nanoparticles for magnetic fluid hyperthermia *J. Magn. Magn. Mater.* **321** 1947–50
[82] Gordon R T, Hines J R and Gordon D 1979 Intracellular hyperthermia—biophysical approach to cancer-treatment via intracellular temperature and biophysical alterations *Med. Hypotheses* **5** 83–102
[83] Goya G F, Asin L and Ibarra M R 2013 Cell death induced by ac magnetic fields and magnetic nanoparticles: current state and perspectives *Int. J. Hyperthermia* **29** 810–8
[84] Gruettner C, Mueller K, Teller J and Westphal F 2013 Synthesis and functionalisation of magnetic nanoparticles for hyperthermia applications *Int. J. Hyperthermia* **29** 777–89
[85] Gruettner C, Mueller K, Teller J, Westphal F, Foreman A and Ivkov R 2007 Synthesis and antibody conjugation of magnetic nanoparticles with improved specific power absorption rates for alternating magnetic field cancer therapy *J. Magn. Magn. Mater.* **311** 181–6
[86] Hall E J and Giaccia A J *Radiobiology for the Radiologist Seventh Ed.* (Phildelphia PA: Lippincott Williams and Wilkins)
[87] Hamad-Schifferli K, Schwartz J J, Santos A T, Zhang S G and Jacobson J M 2002 Remote electronic control of DNA hybridization through inductive coupling to an attached metal nanocrystal antenna *Nature* **415** 152–5
[88] Handy E, Ivkov R, Ellis-Busby D, Foreman A, Braunhut S, Gwost D and Ardman B 2003 Thermotherapy via targeted delivery of nanoscale magnetic particles *US Patent Appl. Publ.* US2003/0032995
[89] Hanggi P, Talkner P and Borkovec M 1990 Reaction-rate theory—50 years after kramers *Rev. Mod. Phys.* **62** 251–341
[90] Hao Y L and Teja A S 2003 Continuous hydrothermal crystallization of alpha-Fe2O3 and Co3O4 nanoparticles *J. Mater. Res.* **18** 415–22
[91] Harvey P R and Katznelson E 1999 Modular gradient coil: a new concept in high-performance whole-body gradient coil design *Magn. Reson. Med.* **42** 561–70
[92] Hasany S F, Abdurahman N H, Sunarti A R and Jose R 2013 Magnetic iron oxide nanoparticles: chemical synthesis and applications review *Curr. Nanosci.* **9** 561–75
[93] Hedayati M *et al* 2013 The effect of cell cluster size on intracellular nanoparticle-mediated hyperthermia: is it possible to treat microscopic tumors? *Nanomedicine* **8** 29–41
[94] Heider F, Dunlop D J and Sugiura N 1987 Magnetic-properties of hydrothermally recrystallized magnetite crystals *Science* **236** 1287–90
[95] Hendriksen P V, Linderoth S and Lindgard P A 1993 Finite-size modification of the magnetic properties of clusters *Phys. Rev.* B **48** 7259–73
[96] Hergt R, Andra W, d'Ambly C G, Hilger I, Kaiser W A, Richter U and Schmidt H G 1998 Physical limits of hyperthermia using magnetite fine particles *IEEE Trans. Magn.* **34** 3745–54
[97] Hergt R and Dutz S 2007 Magnetic particle hyperthermia-biophysical limitations of a visionary tumour therapy *J. Magn. Magn. Mater.* **311** 187–92
[98] Hergt R, Dutz S and Roeder M 2008 Effects of size distribution on hysteresis losses of magnetic nanoparticles for hyperthermia *J. Phys.: Condens. Matter* **20** 385214
[99] Hergt R, Dutz S and Zeisberger M 2010 Validity limits of the Néel relaxation model of magnetic nanoparticles for hyperthermia *Nanotechnology* **21** 015706
[100] Hergt R, Hiergeist R, Hilger I, Kaiser W A, Lapatnikov Y, Margel S and Richter U 2004 Maghemite nanoparticles with very high ac-losses for application in RF-magnetic hyperthermia *J. Magn. Magn. Mater.* **270** 345–57
[101] Hergt R, Hiergeist R, Zeisberger M, Schuler D, Heyen U, Hilger I and Kaiser W A 2005 Magnetic properties of bacterial magnetosomes as potential diagnostic and therapeutic tools *J. Magn. Magn. Mater.* **293** 80–6
[102] Hiergeist R, Andra W, Buske N, Hergt R, Hilger I, Richter U and Kaiser W 1999 Application of magnetite ferrofluids for hyperthermia *J. Magn. Magn. Mater.* **201** 420–2
[103] Hildebrandt B, Wust P, Ahlers O, Dieing A, Sreenivasa G, Kerner T, Felix R and Riess H 2002 The cellular and molecular basis of hyperthermia *Crit. Rev. Oncol. Hematol.* **43** 33–56
[104] Hilger I, Andra W, Hergt R, Hiergeist R and Kaiser W A 2005 Magnetic thermotherapy of breast tumors: an experimental therapeutic approach *Rofo-Fortschritte Auf Dem Gebiet Der Rontgenstrahlen Und Der Bildgebenden Verfahren* **177** 507–15
[105] Hilger I, Andra W, Hergt R, Hiergeist R, Schubert H and Kaiser W A 2001 Electromagnetic heating of breast tumors in interventional radiology: *in vitro* and *in vivo* studies in human cadavers and mice *Radiology* **218** 570–5
[106] Hilger I, Hergt R and Kaiser W A 2000 Effects of magnetic thermoablation in muscle tissue using iron oxide particles—an *in vitro* study *Invest. Radiol.* **35** 170–9

[107] Hilger I, Hiergeist R, Hergt R, Winnefeld K, Schubert H and Kaiser W A 2002 Thermal ablation of tumors using magnetic nanoparticles—an *in vivo* feasibility study *Invest. Radiol.* **37** 580–6

[108] Huang H, Delikanli S, Zeng H, Ferkey D M and Pralle A 2010 Remote control of ion channels and neurons through magnetic-field heating of nanoparticles *Nat. Nanotechnology* **5** 602–6

[109] Huehn D *et al* 2013 Polymer-coated nanoparticles interacting with proteins and cells: focusing on the sign of the net charge *Acs Nano* **7** 3253–63

[110] Hugounenq P *et al* 2012 Iron oxide monocrystalline nanoflowers for highly efficient magnetic hyperthermia *J. Phys. Chem.* **116** 15702–12

[111] Huh D, Bahng J H, Ling Y B, Wei H H, Kripfgans O D, Fowlkes J B, Grotberg J B and Takayama S 2007 Gravity-driven microfluidic particle sorting device with hydrodynamic separation amplification *Anal. Chem.* **79** 1369–76

[112] Hyeon T, Lee S S, Park J, Chung Y and Bin Na H 2001 Synthesis of highly crystalline and monodisperse maghemite nanocrystallites without a size-selection process *J. Am. Chem. Soc.* **123** 12798–801

[113] Hynynen K, Deyoung D, Kundrat M and Moros E 1989 The effect of blood perfusion rate on the temperature distributions induced by multiple, scanned and focused ultrasonic beams in dogs kidneys *invivo Int. J. Hyperthermia* **5** 485–97

[114] Ito A, Shinkai M, Honda H and Kobayashi T 2005 Medical application of functionalized magnetic nanoparticles *J. Biosci. Bioeng.* **100** 1–11

[115] Janko C, Duerr S, Munoz L E, Lyer S, Chaurio R, Tietze R, von Loehneysen S, Schorn C, Herrmann M and Alexiou C 2013 Magnetic drug targeting reduces the chemotherapeutic burden on circulating leukocytes *Int. J Mol Sci.* **14** 7341–55

[116] Jeun M, Lee S, Kang J K, Tomitaka A, Kang K W, Kim Y I, Takemura Y, Chung K W, Kwak J and Bae S 2012 Physical limits of pure superparamagnetic Fe3O4 nanoparticles for a local hyperthermia agent in nanomedicine *Appl. Phys. Lett.* **100** 924061–4

[117] Johannsen M, Gneueckow U, Thiesen B, Taymoorian K, Cho C H, Waldofner N, Scholz R, Jordan A, Loening S A and Wust P 2007 Thermotherapy of prostate cancer using magnetic nanoparticles: feasibility, imaging, and three-dimensional temperature distribution *Eur. Urol.* **52** 1653–62

[118] Johannsen M, Gneveckow U, Taymoorian K, Thiesen B, Waldoefner N, Scholz R, Jung K, Jordan A, Wust P and Loening S A 2007 Morbidity and quality of life during thermotherapy using magnetic nanoparticles in locally recurrent prostate cancer: results of a prospective phase I trial *Int. J. Hyperthermia* **23** 315–23

[119] Johannsen M, Thiesen B, Wust P and Jordan A 2010 Magnetic nanoparticle hyperthermia for prostate cancer *Int. J. Hyperthermia* **26** 790–5

[120] Jordan A, Scholz R, Wust P, Fahling H, Krause J, Wlodarczyk W, Sander B, Vogl T and Felix R 1997 Effects of magnetic fluid hyperthermia (MFH) on C3H mammary carcinoma *in vivo Int. J. Hyperthermia* **13** 587–605

[121] Jordan A, Scholz R, Wust P, Schirra H, Schiestel T, Schmidt H and Felix R 1999 Endocytosis of dextran and silan-coated magnetite nanoparticles and the effect of intracellular hyperthermia on human mammary carcinoma cells *in vitro J. Magn. Magn. Mater.* **194** 185–96

[122] Kalambur V S, Longmire E K and Bischof J C 2007 Cellular level loading and heating of superparamagnetic iron oxide nanoparticles *Langmuir* **23** 12329–36

[123] Kallumadil M, Tada M, Nakagawa T, Abe M, Southern P and Pankhurst Q A 2009 Suitability of commercial colloids for magnetic hyperthermia *J. Magn. Magn. Mater.* **321** 1509–13

[124] Keblinski P, Cahill D G, Bodapati A, Sullivan C R and Taton T A 2006 Limits of localized heating by electromagnetically excited nanoparticles *J. Appl. Phys.* **100** 543051–5

[125] Khalafalla S E and Reimers G W 1980 Preparation of dilution-stable aqueous magnetic fluids *IEEE Trans. Magn.* **16** 178–83

[126] Khandhar A P, Ferguson R M, Simon J A and Krishnan K M 2012 Enhancing cancer therapeutics using size-optimized magnetic fluid hyperthermia *J. Appl. Phys.* **111** 7B3061

[127] Kim D-H, Rozhkova E A, Ulasov I V, Bader S D, Rajh T, Lesniak M S and Novosad V 2010 Biofunctionalized magnetic-vortex microdiscs for targeted cancer-cell destruction *Nat. Mater.* **9** 165–71

[128] Kotitz R, Fannin P C and Trahms L 1995 Time-domain study of brownian and neel relaxation in ferrofluids *J. Magn. Magn. Mater.* **149** 42–6

[129] Kronmueller H and Faehnle M 2003 *Micromagnetism and the Microstructure of Ferromagnetic Solids* (Cambridge: Cambridge University Press)

[130] Kurland H-D, Grabow J, Staupendahl G, Andrae W, Dutz S and Bellemann M E 2007 Magnetic iron oxide nanopowders produced by CO_2 laser evaporation *J. Magn. Magn. Mater.* **311** 73–7

[131] Kurland H-D, Grabow J, Staupendahl G, Müller F A, Müller E, Dutz S and Bellemann M E 2009 Magnetic iron oxide nanopowders produced by CO_2 laser evaporation —'*in situ*' coating and particle embedding in a ceramic matrix *J. Magn. Magn. Mater.* **321** 1381–5

[132] LaConte L, Nitin N and Bao G 2005 Magnetic nanoparticle probes *Nanotoday* **8** 32–8

[133] Landau L D and Lifshitz E M 1960 *Electrodynamics of Continuous Media* (London: Pergamon)

[134] Langevin D 1992 Micelles and microemulsiond *Annu. Rev. Phys. Chem.* **43** 341–69

[135] Lapresta-Fernandez A, Doussineau T, Dutz S, Steiniger F, Moro A J and Mohr G J 2011 Magnetic and fluorescent core–shell nanoparticles for ratiometric pH sensing *Nanotechnology* **22** 415501

[136] Lapresta-Fernandez A, Doussineau T, Moro A J, Dutz S, Steiniger F and Mohr G J 2011 Magnetic core–shell fluorescent pH ratiometric nanosensor using a stober coating method *Anal. Chim. Acta* **707** 164–70

[137] Lartigue L, Hugounenq P, Alloyeau D, Clarke S P, Levy M, Bacri J-C, Bazzi R, Brougham D F, Wilhelm C and Gazeau F 2012 Cooperative organization in iron oxide multi-core nanoparticles potentiates their efficiency as heating mediators and MRI contrast agents *ACS Nano* **6** 10935–49

[138] Laurell T, Petersson F and Nilsson A 2007 Chip integrated strategies for acoustic separation and manipulation of cells and particles *Chem. Soc. Rev.* **36** 492–506

[139] Laurent S, Burtea C, Thirifays C, Rezaee F and Mahmoudi M 2013 Significance of cell 'observer' and protein source in nanobiosciences *J. Colloid Interface Sci.* **392** 431–45

[140] Laurent S, Forge D, Port M, Roch A, Robic C, Elst L V and Muller R N 2008 Magnetic iron oxide nanoparticles: synthesis, stabilization, vectorization, physicochemical characterizations, and biological applications *Chem. Rev.* **108** 2064–110

[141] Leveen H H, Wapnick S, Piccone V, Falk G and Ahmed N 1976 Tumor eradication by radiofrequency therapy—response in 21 patients *J. Am. Med. Assoc.* **235** 2198–200

[142] Levy M *et al* 2011 Correlating magneto-structural properties to hyperthermia performance of highly monodisperse iron oxide nanoparticles prepared by a seeded-growth route *Chem. Mater.* **23** 4170–80

[143] Li Z, Kawashita M, Araki N, Mitsumori M, Hiraoka M and Doi M 2011 Preparation of magnetic iron oxide

nanoparticles for hyperthermia of cancer in a FeCl2-NaNO3-NaOH aqueous system *J. Biomater. Appl.* **25** 643–61
[144] Lohrke J, Briel A and Maeder K 2008 Characterization of superparamagnetic iron oxide nanoparticles by asymmetrical flow-field-flow-fractionation *Nanomedicine* **3** 437–52
[145] Lubbe A S *et al* 1996 Clinical experiences with magnetic drag targeting: a phase I study with 4′-epidoxorubicin in 14 patients with advanced solid tumors *Cancer Res.* **56** 4686–93 http://cancerres.aacrjournals.org/content/56/20/4686.full.pdf+html
[146] Lundqvist M, Stigler J, Elia G, Lynch I, Cedervall T and Dawson K A 2008 Nanoparticle size and surface properties determine the protein corona with possible implications for biological impacts *Proc. Natl. Acad. Sci. USA* **105** 14265–70
[147] Magforce A G press release, 31 March 2014 (available at: www.magforce.de/presse-investoren/news-events/detail/article/einschluss-des-ersten-patienten-in-der-glioblastom-studie-mf-1001-im-universitaetsklinikum-muenster.html)
[148] Mahmoudi M *et al* 2013 Temperature: the 'Ignored' factor at the nanobio interface *Acs Nano* **7** 6555–62
[149] Maier-Hauff K, Ulrich F, Nestler D, Niehoff H, Wust P, Thiesen B, Orawa H, Budach V and Jordan A 2011 Efficacy and safety of intratumoral thermotherapy using magnetic iron-oxide nanoparticles combined with external beam radiotherapy on patients with recurrent glioblastoma multiforme *J. Neurooncol.* **103** 317–24
[150] Massart R 1980 Preparation of aqueous ferrofluids without using surfactant—behavior as a function of the pH and the counterions *C. R. Hebd. Seances Acad. Sci.* C **291** 1–3
[151] Mee C D and Daniel E D 1996 *Magnetic Recording Technology* McGraw-Hill) (NewYork:
[152] Mi Y, Liu X, Zhao J, Ding J and Feng S-S 2012 Multimodality treatment of cancer with herceptin conjugated, thermomagnetic iron oxides and docetaxel loaded nanoparticles of biodegradable polymers *Biomaterials* **33** 7519–29
[153] Milne G, Rhodes D, MacDonald M and Dholakia K 2007 Fractionation of polydisperse colloid with acousto-optically generated potential energy landscapes *Opt. Lett.* **32** 1144–6
[154] Moras K, Schaarschuch R, Riehemann W, Zinoveva S, Modrow H and Eberbeck D 2005 Production and characterisation of magnetic nanoparticles produced by laser evaporation for ferrofluids *J. Magn. Magn. Mater.* **293** 119–26
[155] Moroz P, Jones S K and Gray B N 2002 Magnetically mediated hyperthermia: current status and future directions *Int. J. Hyperthermia* **18** 267–84
[156] Mueller R, Dutz S, Habisreuther T and Zeisberger M 2011 Investigations on magnetic particles prepared by cyclic growth *J. Magn. Magn. Mater.* **323** 1223–7
[157] Mueller R, Dutz S, Neeb A, Cato A C B and Zeisberger M 2013 Magnetic heating effect of nanoparticles with different sizes and size distributions *J. Magn. Magn. Mater.* **328** 80–5
[158] Muerbe J, Rechtenbach A and Toepfer J 2008 Synthesis and physical characterization of magnetite nanoparticles for biomedical applications *Mater. Chem. Phys.* **110** 426–33
[159] Mustin B and Stoeber B 2010 Deposition of particles from polydisperse suspensions in microfluidic systems *Microfluid. Nanofluid.* **9** 905–13
[160] Néel L 1949 Influence des fluctuations thermiques a l'aimantation des particules ferromagnetiques *C.R. Dir. Rec. Sci.* **228** 664–8
[161] Niira K 1960 Temperature dependence of the magnetization of dysprosium metal *Phys. Rev.* **117** 129–33
[162] Nikolajski M, Wotschadlo J, Clement J H and Heinze T 2012 Amino-functionalized cellulose nanoparticles: preparation, characterization, and interactions with living cells *Macromol. Biosci.* **12** 920–5
[163] Nyborg W L 1988 Solutions of the bio-heat transfer equation *Phys. Med. Biol.* **33** 785–92
[164] Odenbach S 2002 *Ferrofluids—Magnetically Controllable Fluids and their Applications; (Lecture notes in Physics)* (Berlin: Springer) *Bd594*
[165] Okabe K, Inada N, Gota C, Harada Y, Funatsu T and Uchiyama S 2012 Intracellular temperature mapping with a fluorescent polymeric thermometer and fluorescence lifetime imaging microscopy *Nat. Commun.* **3** 705
[166] Okoli C, Sanchez-Dominguez M, Boutonnet M, Jaras S, Civera C, Solans C and Kuttuva G R 2012 Comparison and functionalization study of microemulsion-prepared magnetic iron oxide nanoparticles *Langmuir* **28** 8479–85
[167] Orte A, Alvarez-Pez J M and Ruedas-Rama M J 2013 Fluorescence lifetime imaging microscopy for the detection of intracellular pH with quantum dot nanosensors *Acs Nano* **7** 6387–95
[168] Ortega D and Pankhurst Q A 2013 *Nanoscience* ed P O'Brien (Cambridge: Royal Society of Chemistry) pp 60–88
[169] Osuna J, deCaro D, Amiens C, Chaudret B, Snoeck E, Respaud M, Broto J M and Fert A 1996 Synthesis, characterization, and magnetic properties of cobalt nanoparticles from an organometallic precursor *J. Phys. Chem.* **100** 14571–4
[170] Pamme N 2007 Continuous flow separations in microfluidic devices *Lab Chip* **7** 1644–59
[171] Pamme N, Eijkel J C T and Manz A 2006 On-chip free-flow magnetophoresis: Separation and detection of mixtures of magnetic particles in continuous flow *J. Magn. Magn. Mater.* **307** 237–44
[172] Pankhurst Q A, Thanh N T K, Jones S K and Dobson J 2009 Progress in applications of magnetic nanoparticles in biomedicine *J. Phys. D: Appl. Phys.* **42** 224001
[173] Park J *et al* 2005 One-nanometer-scale size-controlled synthesis of monodisperse magnetic iron oxide nanoparticles *Angew. Chem.-Int. Ed.* **44** 2872–7
[174] Petrosyan A K and Mirzakhanyan A A 1986 Zero-field splitting and G-values of D8 ions in a trigonal crystal-field *Phys. Status Solidi b* **133** 315–9
[175] Petryk A A, Giustini A J, Gottesman R E, Kaufman P A and Hoopes P J 2013 Magnetic nanoparticle hyperthermia enhancement of cisplatin chemotherapy cancer treatment *Int. J. Hyperthermia* **29** 845–51
[176] Pollert E and Záveta K 2012 *Magnetic Nanoparticles: From Fabrication to Clinical Applications* ed N T K Thanh (London: CRC Press) pp 449–79
[177] Rabin Y 2002 Is intracellular hyperthermia superior to extracellular hyperthermia in the thermal sense? *Int. J. Hyperthermia* **18** 194–202
[178] Rand R W, Snow H D, Elliott D G and Haskins G M 1985 *Induction heating method for use in causing necrosis of Neoplasm.* US Patent 4.545.368
[179] Reilly J P 1998 *Applied Bioelectricity: From Electrical Stimulation to Electro Pathology* (New York: Springer)
[180] Richter H, Kettering M, Wiekhorst F, Steinhoff U, Hilger I and Trahms L 2010 Magnetorelaxometry for localization and quantification of magnetic nanoparticles for thermal ablation studies *Phys. Med. Biol.* **55** 623–33
[181] Riedinger A, Guardia P, Curcio A, Garcia M A, Cingolani R, Manna L and Pellegrino T 2013 Subnanometer local temperature probing and remotely controlled drug release based on azo-functionalized iron oxide nanoparticles *Nano Lett.* **13** 2399–406
[182] Robins H I *et al* 1997 Phase I clinical trial of melphalan and 41.8 degrees C whole-body hyperthermia in cancer patients *J. Clin. Oncol.* **15** 158–64 http://jco.ascopubs.org/content/15/1/158.full.pdf+html
[183] Rodrigues H F, Mello F M, Branquinho L C, Zufelato N, Silveira-Lacerda E P and Bakuzis A F 2013 Real-time

infrared thermography detection of magnetic nanoparticle hyperthermia in a murine model under a non-uniform field configuration *Int. J. Hyperthermia* **29** 752–67
[184] Rodrigues P A M, Yu P Y, Tamulaitis G and Risbud S H 1996 Laser-induced heating of nanocrystals embedded in glass matrices *J. Appl. Phys.* **80** 5963–6
[185] Roggan A, Beuthan J, Schruender S and Mueller G 1999 Diagnostik und therapie mit dem laser *Phys. Bl.* **55** 25–30
[186] Rosensweig R E 2002 Heating magnetic fluid with alternating magnetic field *J. Magn. Magn. Mater.* **252** 370–4
[187] Salazar-Alvarez G *et al* 2008 Cubic versus spherical magnetic nanoparticles: the role of surface anisotropy *J. Am. Chem. Soc.* **130** 13234–9
[188] Salloum M, Ma R and Zhu L 2009 Enhancement in treatment planning for magnetic nanoparticle hyperthermia: optimization of the heat absorption pattern *Int. J. Hyperthermia* **25** 309–21
[189] Schaller V, Wahnstrom G, Sanz-Velasco A, Enoksson P and Johansson C 2009 Monte Carlo simulation of magnetic multi-core nanoparticles *J. Magn. Magn. Mater.* **321** 1400–3
[190] Schaller V, Wahnstrom G, Sanz-Velasco A, Gustafsson S, Olsson E, Enoksson P and Johansson C 2009 Effective magnetic moment of magnetic multicore nanoparticles *Phys. Rev. B* **80** 924061–4
[191] Scheffel A, Gruska M, Faivre D, Linaroudis A, Plitzko J M and Schuler D 2006 An acidic protein aligns magnetosomes along a filamentous structure in magnetotactic bacteria *Nature* **440** 110–4
[192] Schueler D 1999 Formation of magnetosomes in magnetotactic bacteria *J. Mol. Microbiol. Biotechnol.* **1** 79–86
[193] Schueler D and Frankel R B 1999 Bacterial magnetosomes: microbiology, biomineralization and biotechnological applications *Appl. Microbiol. Biotechnol.* **52** 464–73
[194] Schweiger C, Hartmann R, Zhang F, Parak W J, Kissel T H and Rivera Gil P 2012 Quantification of the internalization patterns of superparamagnetic iron oxide nanoparticles with opposite charge *J. Nanobiotechnol.* **10** 28
[195] Serantes D *et al* 2010 Influence of dipolar interactions on hyperthermia properties of ferromagnetic particles *J. Appl. Phys.* **108** 073918
[196] Shliomis M I and Stepanov V I 1994 Theory of dynamic susceptibility of magnetic fluids *Adv. Chem. Phys.* **87** 1–30
[197] Smistrup K, Hansen O, Bruus H and Hansen M F 2005 Magnetic separation in microfluidic systems using microfabricated electromagnets-experiments and simulations *J. Magn. Magn. Mater.* **293** 597–604
[198] Sollier E, Rostaing H, Pouteau P, Fouillet Y and Achard J L 2009 Passive microfluidic devices for plasma extraction from whole human blood *Sensors Actuators* B **141** 617–24
[199] Sonnenschein R and Gross J 1986 Temperature field computation for radiofrequency heating of deep-seated tumors *Recent Results Cancer Res.* **101** 132–7
[200] Stiller W 1989 *Arrhenius Equation and Non-Equilibrium Kinetics, in Teubner: Texte Zur Physik, Band 21* (Weinheim: VCH)
[201] Stoetzel C, Kurland H-D, Grabow J, Dutz S, Mueller E, Sierka M and Mueller F A 2013 Control of the crystal phase composition of FexOy nanopowders prepared by CO2 laser vaporization *Cryst. Growth Des.* **13** 4868–76
[202] Stoner E C and Wohlfarth E P 1948 A mechanism of magnetic hysteresis in heterogeneous alloys *Phil. Trans. R. Soc.* A **240** 599–642
[203] Strohbehn J W, Bowers E D, Walsh J E and Douple E B 1979 Invasive microwave antenna for locally-induced hyperthermia for cancer-therapy *J. Microw. Power Electromagn. Energy* **14** 339–50
[204] Tartaj P, Morales M D, Veintemillas-Verdaguer S, Gonzalez-Carreno T and Serna C J 2003 The preparation of magnetic nanoparticles for applications in biomedicine *J. Phys. D: Appl. Phys.* **36** R182–97
[205] Taupitz M, Schmitz S and Hamm B 2003 Superparamagnetic iron oxide particles: current state and future development *Rofo-Fortschritte Auf Dem Gebiet Der Rontgenstrahlen Und Der Bildgebenden Verfahren* **175** 752–65
[206] Taylor L S 1980 Implantable radiators for cancer-therapy by microwave hyperthermia *Proc. IEEE* **68** 142–9
[207] Tenzer S *et al* 2011 Nanoparticle size is a critical physicochemical determinant of the human blood plasma corona: a comprehensive quantitative proteomic analysis *Acs Nano* **5** 7155–67
[208] Thiesen B and Jordan A 2008 Clinical applications of magnetic nanoparticles for hyperthermia *Int. J. Hyperthermia* **24** 467–74
[209] Thomas L A, Dekker L, Kallumadil M, Southern P, Wilson M, Nair S P, Pankhurst Q A and Parkin I P 2009 Carboxylic acid-stabilised iron oxide nanoparticles for use in magnetic hyperthermia *J. Mater. Chem.* **19** 6529–35
[210] Thrall D E *et al* 2012 Thermal dose fractionation affects tumour physiological response *Int. J. Hyperthermia* **28** 431–40
[211] Thurm S and Odenbach S 2002 Magnetic separation of ferrofluids *J. Magn. Magn. Mater.* **252** 247–9
[212] Timko M *et al* 2013 Hyperthermic effect in suspension of magnetosomes prepared by various methods *IEEE Trans. Magn.* **49** 250–4
[213] Toraya-Brown S, Sheen M R, Baird J R, Barry S, Demidenko E, Turk M J, Hoopes P J, Conejo-Garcia J R and Fiering S 2013 Phagocytes mediate targeting of iron oxide nanoparticles to tumors for cancer therapy *Integr. Biol.* **5** 159–71
[214] Urtizberea A, Natividad E, Arizaga A, Castro M and Mediano A 2010 Specific absorption rates and magnetic properties of ferrofluids with interaction effects at low concentrations *J. Phys. Chem.* C **114** 4916–22
[215] van der Zee J 2002 Heating the patient: a promising approach? *Ann. Oncol.* **13** 1173–84
[216] Veiseh O, Kievit F M, Gunn J W, Ratner B D and Zhang M 2009 A ligand-mediated nanovector for targeted gene delivery and transfection in cancer cells *Biomaterials* **30** 649–57
[217] Wang H, Li X, Xi X, Hu B, Zhao L, Liao Y and Tang J 2011 Effects of magnetic induction hyperthermia and radiotherapy alone or combined on a murine 4T1 metastatic breast cancer model *Int. J. Hyperthermia* **27** 563–72
[218] Weissleder R, Stark D D, Engelstad B L, Bacon B R, Compton C C, White D L, Jacobs P and Lewis J 1989 Superparamagnetic iron-oxide—pharmacokinetics and toxicity *Am. J. Roentgenol.* **152** 167–73
[219] Witt A, Fabian K and Bleil U 2005 Three-dimensional micromagnetic calculations for naturally shaped magnetite: octahedra and magnetosomes *Earth Planet. Sci. Lett.* **233** 311–24
[220] Wotschadlo J *et al* 2009 Magnetic nanoparticles coated with carboxymethylated polysaccharide shells—Interaction with human cells *J. Magn. Magn. Mater.* **321** 1469–73
[221] Wust P, Hildebrandt B, Sreenivasa G, Rau B, Gellermann J, Riess H, Felix R and Schlag P M 2002 Hyperthermia in combined treatment of cancer *Lancet Oncol.* **3** 487–97
[222] Xu C and Teja A S 2008 Continuous hydrothermal synthesis of iron oxide and PVA-protected iron oxide nanoparticles *J. Supercrit. Fluids* **44** 85–91
[223] Yamada K *et al* 2010 Minimally required heat doses for various tumour sizes in induction heating cancer therapy determined by computer simulation using experimental data *Int. J. Hyperthermia* **26** 465–74
[224] Yamada M and Seki M 2005 Hydrodynamic filtration for on-chip particle concentration and classification utilizing microfluidics *Lab Chip* **5** 1233–9

[225] Yang J-M, Yang H and Lin L 2011 Quantum dot nano thermometers reveal heterogeneous local thermogenesis in living cells *ACS Nano* **5** 5067–71

[226] Yuan Y and Borca-Tasciuc D-A 2013 Anomalously high specific absorption rate in bioaffine ligand-coated iron oxide nanoparticle suspensions *IEEE Trans. Magn.* **49** 263–8

[227] Yuan Y, Rende D, Altan C L, Bucak S, Ozisik R and Borca-Tasciuc D-A 2012 Effect of surface modification on magnetization of iron oxide nanoparticle colloids *Langmuir* **28** 13051–9

[228] Zborowski M, Sun L P, Moore L R, Williams P S and Chalmers J J 1999 Continuous cell separation using novel magnetic quadrupole flow sorter *J. Magn. Magn. Mater.* **194** 224–30

[229] Zeisberger M, Dutz S, Lehnert J and Muller R 2009 Measurement of the distribution parameters of size and magnetic properties of magnetic nanoparticles for medical applications *J. Phys.: Conf. Ser.* **149** 012115

[230] Zeng Q, Baker I, Loudis J A, Liao Y, Hoopes P J and Weaver J B 2007 Fe/Fe oxide nanocomposite particles with large specific absorption rate for hyperthermia *Appl. Phys. Lett.* **90** 233112

[231] Zhang J, Dewilde A H, Chinn P, Foreman A, Barry S, Kanne D and Braunhut S J 2011 Herceptin-directed nanoparticles activated by an alternating magnetic field selectively kill HER-2 positive human breast cells *in vitro* via hyperthermia *Int. J. Hyperthermia* **27** 682–97